DEPARTAMENTO DE ECUACIONES DIFERENCIALES Y ANÁLISIS NUMÉRICO

Ecuaciones de coordenadas colectivas para una ecuación de tipo sine-Gordon. Análisis de fenómenos tipo ratchet en solitones topológicos

A Project Report Submitted in Partial Fulfilment of the Requirements for the Degree of
MÁSTER UNIVERSITARIO DE MATEMÁTICAS

Author: Faustino Palmero Ramos

Supervisors: Jesús Cuevas Maraver, Francisco Guillén González

FACULTAD DE MATEMÁTICAS

UNIVERSIDAD DE SEVILLA

JUNIO 2022

Acknowledgements

I would like to thank my supervisors, Professor Jesús Cuevas Maraver from the Department of Applied Physics I and Professor Francisco Guillén González from the Department of Differential Equations and Numerical Analysis at the University of Seville, for their guidance and support throughout the duration of the project. I would also like to thank the "Ministerio de Educación y Formación Profesional" for granting me the "Beca de Colaboración" to conduct this work.

Faustino Palmero Ramos

June 2022

Abstract

The main aim of this project is to study the so-called soliton ratchet phenomena in a Frenkel-Kontorova model, by making use of the collective coordinate approximation. From a mathematical point of view, the discrete double sine-Gordon equation will be considered. This system, which consists of N coupled second-order ordinary differential equations (ODEs), will be reduced to a system of just two coupled second-order ODEs, in terms of the collective coordinates, that is, the center of mass $X(t)$ and the width $l(t)$ of the topological soliton, or kink, solution. Once these equations are obtained, the aim is to look at whether the different motion regimes that this reduced system show adequately approximate the full system.

Resumen

El objetivo principal de este proyecto es estudiar el llamado fenómeno ratchet de solitones en un modelo de Frenkel-Kontorova, haciendo uso de la aproximación de coordenadas colectivas. Se estudiará la ecuación discreta de doble sine-Gordon desde un punto de vista matemático. Este sistema, que está formado por N ecuaciones diferenciales ordinarias (EDO) acopladas de segundo orden, se reducirá a un sistema de solo dos EDOs acopladas de segundo orden en términos de las coordenadas colectivas, es decir, el centro de masa $X(t)$ y la anchura $l(t)$ de la solución de solitón topológico, también llamada kink. Una vez obtenidas estas ecuaciones, el objetivo es ver si los diferentes regímenes de movimiento que muestra este sistema reducido se aproximan adecuadamente al sistema completo.

Contents

Chapter 1

Introduction

The sine-Gordon equation is one of the most renowned non-linear differential equation models. This equation is obtained by taking the regular Klein-Gordon equation, and replacing the linear potential term by a non-linear sine term, i.e.:

$$\phi_{tt} + \sin\phi - \Delta\phi = 0. \tag{1.1}$$

The popularity of this equation is due to the large number of applications, starting in the 1860s with the study of surfaces of constant negative curvature (*pseudospheres*) in space, and later being rediscovered in the 1930s, in its discrete version – known as the Frenkel-Kontorova, or discrete sine-Gordon model–, by Frenkel and Kontorova when studying dislocations in crystal lattices [1], and was later used to describe a chain of coupled pendula [2]. The Frenkel-Kontorova model regained interest in the 1990s with its use in the theory of *Josephson junctions* arrays in the study of parallel layers of superconductors. More recently, this model has been used to study galactic orbits near the inner Lindblad resonance [1, 3], as well as to describe the dynamics of molecular motion in nematic liquid crystals under a twisting disturbance of the molecular arrangement under the external electric field [4]. Apart from the large number of applications that this equation has, it is by itself mathematically relevant due to its particular structure and its properties. In particular, the complete integrability of the system, which implies the possibility of finding conserved quantities and exact analytical solutions to the equation. Of particular physical importance among these solutions are solitons, or solitary waves, which are spatially localized travelling waves whose shape is maintained in time. These types of solutions were first discovered in the late 19th century via the so-called Bäcklund transformations and were called kinks, or topological solitons [1, 5, 6]. The importance of solitons as solutions to this equation is however not limited to the realm of Physics. They have been widely recognized to take part in many biological

interactions, and in particular the Frenkel-Kontorova has been used to model DNA chains, implying that soliton excitations may exist in these chains [7].

In addition to the sine-Gordon equation, one can consider a slight variation of it by adding a second non-linear term, typically another periodic term, which also permits to find kinks, since in order for these to exist the potential must possess at least two minima. This leads to the double sine-Gordon equation, written as:

$$\phi_{tt} - \Delta\phi + \sin\phi + \lambda\cos 2\phi = 0.$$

Throughout this project, we will not be interested in studying the continuous sine-Gordon equation or its variant, but the analogous discrete system. As mentioned before, this system was first introduced by Frenkel and Kontorova in the theory of crystal dislocations. Denoting by n the lattice nodes, by N the number of lattice nodes, and by h the distance between these nodes in the lattice, we can write this system as:

$$\ddot{\phi}_n - \kappa\Delta_d\phi_n + \sin\phi_n = 0, \qquad n = 1, \dots, N, \tag{1.2}$$

where $\kappa = 1/h^2$, and Δ_d denotes the discrete Laplacian. In 1D, this is $\Delta_d\phi_n = \phi_{n+1} - 2\phi_n + \phi_{n-1}$. One can see that, by taking the continuous limit $h \to 0$, we recover (1.1), with continuous coordinate $x = n/\sqrt{\kappa}$. Similarly, we can consider different types of potentials on this system, in particular we can add another periodic term to obtain the discrete analogous to the double sine-Gordon equation:

$$\ddot{\phi}_n - \kappa\Delta_d\phi_n + \sin\phi_n + \lambda\cos 2\phi_n = 0, \qquad n = 1, \dots, N. \tag{1.3}$$

This system can be interpreted as a chain of coupled double pendula [8].

The main aim of this project is to study the so-called ratchet phenomenon in topological solitons (i.e. kinks), that is, the emergence of net motion of the soliton under forces of zero average (e.g. a sinusoidal driving force) [1]. This has been extensively studied in the last decades, and it has been predicted via the breaking of the symmetries of the system [9, 10, 11, 12, 13]. The ratchet phenomenon has been observed to appear in non-linear systems like (1.2), both experimentally and in simulations, when space-time symmetries are broken [1, 14, 15, 16, 17, 18]. Examples of such symmetry breakings can be seen by adding a force term to (1.2) made up of two *different* harmonics (e.g. $F(t) = \sin(t) + \cos(2t)$) [19, 20, 21], or by adding another periodic term to the potential [1, 9]. This second case would correspond to having $\lambda \neq 0$ in (1.3). A spatially asymmetric ratchet model was first proposed by Smoluchowski and Feynman [22], and further models have been proposed to describe different situations, such as artificial molecular motors [23], or pearl growth [24]. Additionally, the emergence of ratchet transport when symmetries are broken by time-dependent forces has

been experimentally observed in the case of motion of fluxons in Josephson junctions [15, 17], or currents in semiconductors [25]. The aim of this project is to study the ratchet phenomenon in the particular case of the damped and driven double sine-Gordon equation [1]. However, we will not be studying this system as is, directly, since this has already been done extensively (cf. [26]). We aim to first approximate this system of N second-order ODEs by a simpler system of two second-order ODEs, using so-called collective coordinates [27, 28]. Since our aim is to study kink motion, the collective coordinates that will be introduced are $X(t)$, the center of mass of the kink, and $l(t)$, its width. It is worth noting that even though this will lead to an approximate system, by reducing the number of equations to 2 second-order ODEs the problem will become significantly more manageable and, in certain cases, it will be possible to obtain some analytical results. Once we approximate our system this way, the different types of motion that the kink can exhibit will be studied, depending on the lattice/discretization parameter κ, and on the amplitude of the force applied on the system. Finally, these results will be compared with those obtained in [28] and [26] for the full system with N second-order ODEs.

Chapter 2

Mathematical Background

In this chapter, the equations to be used are introduced, as well as the collective coordinates and the method that is going to be used to approximate the system by a simpler system of two second-order ODEs.

2.1 Discrete sine-Gordon system

We start by considering a set of N forced and damped coupled non-linear oscillators. The dynamics of this system, under a potential V, can be described by the following system of second-order ODEs:

$$\ddot{\phi}_n - \kappa \Delta_d \phi_n + \frac{dV(\phi_n)}{d\phi_n} = -\alpha \dot{\phi}_n + F(t), \qquad n = 1, \ldots, N, \tag{2.1}$$

where ϕ_n is a scalar field, $\dot{\phi}_n$ its time derivative, $\Delta_d \phi_n := \phi_{n+1} + \phi_{n-1} - 2\phi_n$ is the discrete Laplacian, $\kappa = 1/h^2$ is the coupling constant, with h the lattice spacing, α is the damping parameter, $\frac{dV(\phi_n)}{d\phi_n}$ is the derivative of the potential $V(\phi_n)$, and $F(t)$ is a time-periodic external driving. Our aim is to study the ratchet phenomenon, in a kink-type solution. In order to do so, we will need both $F(t)$ and $\frac{dV(\phi_n)}{d\phi_n}$ to be periodic and have zero average (i.e. integrating over time – for $F(t)$ – or over space – since the system is discrete, by adding over n for $\frac{dV(\phi_n)}{d\phi_n}$ – yields 0), and hence for simplicity we will be assuming these are superpositions of trigonometric functions of different periods. In addition to this, it is necessary for these functions to break either the space symmetry (in the case of $\frac{dV(\phi_n)}{d\phi_n}$), or the time symmetry

(in the case of $F(t)$), so that the ratchet phenomenon can appear. To do so, it is assumed that at least one of these two functions is the sum of two (different) harmonics.

Our aim, in order to study the dynamics of a kink-type solution to this system, is to introduce a Collective Coordinates (CC) approximation, so that we can reduce (2.1) from N coupled second-order ODEs to just two of them. In particular, these coordinates will be the center of mass of the kink, $X(t)$, and its width, $l(t)$. Since we are interested in kink-type solutions, the ansatz to be used for (2.1) will be a discrete version of the so-called Rice ansatz for a continuous sine-Gordon equation, $\phi(x) = 4\arctan(\exp(x))$, as used in [29]. This continuous ansatz can be seen in Fig. 2.1.

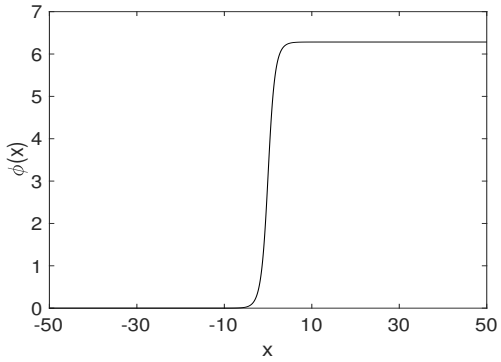

Figure 2.1: Rice ansatz $\phi(x)$ for the continuous sine-Gordon equation.

Discretizing this function in x using the collective coordinates yields the following ansatz for (2.1):

$$\phi_n(t) = 4\arctan(\exp(\theta_n(X(t), l(t)))), \tag{2.2}$$

where $\theta_n(X(t), l(t)) = \frac{n\kappa^{-1/2} - X(t)}{l(t)}$.

2.2 Generalized Travelling-Wave method. Application to the discrete double sine-Gordon model

To derive the equations of motion for the CCs we will use the so-called Generalized Travelling-Wave method (GTWM), first introduced in a general way in [27], and used here as described in [28]. This method consists of first substituting the proposed ansatz into (2.1). Since we are

considering two different coordinates, $X(t)$ and $l(t)$, we will multiply the resulting equations by $\frac{\partial \phi_n}{\partial X}$ and by $\frac{\partial \phi_n}{\partial l}$, respectively. We will from this point onwards call the equation multiplied by $\frac{\partial \phi_n}{\partial X}$ the "equation for $X(t)$", and the equation multiplied by $\frac{\partial \phi_n}{\partial l}$ the "equation for $l(t)$". We note however that both equations will have terms in both $X(t)$ and $l(t)$, and possibly their time derivatives. Finally, to obtain the two second order ODEs for $X(t)$ and $l(t)$, we will add over all of the elements n of the lattice.

As an application of this method, a potential of the form $V(\phi_n) = -\cos(\phi_n) + \frac{\lambda}{2}\sin(2\phi_n)$ is considered, where $\lambda = 0$ in the case of the symmetric potential, and $\lambda \neq 0$ for the asymmetric potential case. We recall that, as previously mentioned, the first case $\lambda = 0$ will imply that the force $F(t)$ in (2.1) is necessarily the superposition of two different harmonics, and for $\lambda \neq 0$ this is not necessary. Additionally, the amplitude of the force must be small so that the collective coordinate approximation is valid; in particular, it may not exceed 0.1. The aim in this section is to reproduce the calculations performed in [28].

To derive the collective coordinate equations, let us consider a generic ansatz of the form $\phi_n(t) \equiv \phi(\theta_n(X(t), l(t)))$, where $\theta_n(X(t), l(t)) = \frac{n\kappa^{-1/2} - X(t)}{l(t)}$. We will see later on why it is convenient to derive the CC equations in terms of a generic ansatz instead of using a more explicit one from the beginning. To plug this into (2.1), we first need to obtain an expression of $\dot{\phi_n}$ and $\ddot{\phi_n}$ in terms of θ_n. For the first derivative we obtain:

$$\begin{aligned}\dot{\phi_n} &= \dot{\theta_n}\frac{d\phi}{d\theta_n}(\theta_n), \\ &= -\frac{\dot{X} + \dot{l}\theta_n}{l}\frac{d\phi}{d\theta_n}(\theta_n),\end{aligned}$$

and for the second derivative we get:

$$\begin{aligned}\ddot{\phi_n} &= \frac{d^2\phi}{d\theta_n^2}\left(\frac{d\theta_n}{dt}\right)^2 + \frac{d\phi}{d\theta_n}\frac{d^2\theta_n}{dt^2}, \\ &= \left(\frac{\dot{X} + \dot{l}\theta_n}{l}\right)^2 \frac{d^2\phi}{d\theta_n^2} + \frac{d\phi}{d\theta_n}\left(\frac{2\dot{X}\dot{l} - l\ddot{X} - l\theta_n\ddot{l} + 2\theta_n\dot{l}^2}{l^2}\right), \\ &= \frac{d^2\phi}{d\theta_n^2}\left(\frac{\dot{X}^2 + \dot{l}^2\theta_n^2 + 2\dot{X}\dot{l}\theta_n}{l}\right) + \frac{d\phi}{d\theta_n}\left(\frac{2\dot{X}\dot{l} - l\ddot{X} - l\theta_n\ddot{l} + 2\theta_n\dot{l}^2}{l^2}\right).\end{aligned}$$

Finally, in addition to these time derivatives, it may be observed that in (2.1) the discrete Laplacian $\Delta_d\phi_n$ appears, which is an expression in terms of ϕ_{n-1}, ϕ_n and ϕ_{n+1}. Hence, before substituting ϕ_n into (2.1), it will be approximated so that it is only expressed in terms of

ϕ_n. To do so we will Taylor expand each of $\phi_{n\pm1}$. In terms of θ_n, we have $\phi_{n\pm1} = \phi(\theta_n \pm \delta)$, where $\delta = 1/(\sqrt{\kappa} l) = h/l$, with h being the spacing of the lattice, and hence considering their Taylor expansion around $\delta = 0$ up to the fourth order term, we have:

$$\phi(\theta_n \pm \delta) \approx \phi(\theta_n) \pm \phi'(\theta_n)\delta + \frac{1}{2}\phi''(\theta_n)\delta^2 \pm \frac{1}{3!}\phi^{(3)}(\theta_n)\delta^3 + \frac{1}{4!}\phi^{(4)}(\theta_n)\delta^4.$$

Therefore, computing $\phi_{n+1} + \phi_{n-1} - 2\phi_n$ we obtain, up to fourth order:

$$\begin{aligned}\phi_{n+1} + \phi_{n-1} - 2\phi_n &\approx \phi(\theta_n) + \phi'(\theta_n)\delta + \frac{1}{2}\phi''(\theta_n)\delta^2 + \frac{1}{3!}\phi^{(3)}(\theta_n)\delta^3 + \frac{1}{4!}\phi^{(4)}(\theta_n)\delta^4 \\ &\quad + \phi(\theta_n) - \phi'(\theta_n)\delta + \frac{1}{2}\phi''(\theta_n)\delta^2 - \frac{1}{3!}\phi^{(3)}(\theta_n)\delta^3 + \frac{1}{4!}\phi^{(4)}(\theta_n)\delta^4 - 2\phi_n(\theta_n), \\ &\approx \phi''(\theta_n)\delta^2 + \frac{1}{12}\phi^{(4)}(\theta_n)\delta^4.\end{aligned}$$

Hence, since $\kappa = 1/(\delta^2 l^2)$, the discrete Laplacian term $-\kappa \Delta_d \phi_n$ will be:

$$-\kappa \Delta_d \phi_n = -\frac{1}{l^2}\phi''(\theta_n) - \frac{1}{12\kappa l^4}\phi^{(4)}(\theta_n).$$

Therefore, an approximation of system (2.1), written in terms of the ansatz ϕ_n and the collective coordinates, is the following:

$$\begin{aligned}C_n^1\frac{\dot{X}^2}{l^2} + C_n^2\frac{\dot{l}^2}{l^2} + C_n^3\frac{2\dot{X}\dot{l}}{l^2} + C_n^4\left(\frac{2\dot{X}\dot{l}}{l^2} - \frac{\ddot{X}}{l}\right) + C_n^5\left(\frac{2\dot{l}^2}{l^2} - \frac{\ddot{l}}{l}\right) - \frac{1}{l^2}C_n^1 \\ - \frac{1}{12\kappa l^4}C_n^6 + C_n^7 + \lambda C_n^8 = \alpha\frac{\dot{X}}{l}C_n^4 + \alpha\frac{\dot{l}}{l}C_n^5 + F(t),\end{aligned} \tag{2.3}$$

where C_n^i are the following functions of $\phi(\theta_n)$ and its derivatives:

$$\begin{aligned}C_n^1 &= \phi''(\theta_n), \\ C_n^2 &= \phi''(\theta_n)\theta_n^2, \\ C_n^3 &= \phi''(\theta_n)\theta_n, \\ C_n^4 &= \phi'(\theta_n),\end{aligned} \qquad \begin{aligned}C_n^5 &= \phi'(\theta_n)\theta_n, \\ C_n^6 &= \phi^{(4)}(\theta_n), \\ C_n^7 &= \sin(\phi(\theta_n)), \\ C_n^8 &= \cos(2\phi(\theta_n)),\end{aligned}$$

Now that (2.1) is written in terms of the ansatz $\phi(\theta_n)$, we can proceed with the GTWM method to obtain the collective coordinate equations.

We start by deriving the equation for $X(t)$. To do so, it is first worth noting the following relation:

$$\begin{aligned}\frac{\partial \phi_n}{\partial X} &= \frac{\partial \theta_n}{\partial X}\frac{d\phi_n}{d\theta_n}, \\ &= -\frac{1}{l(t)}\frac{d\phi_n}{d\theta_n}.\end{aligned}$$

Hence, multiplying (2.3) by this, we obtain the following equation (note that $l(t) \neq 0$, and hence both sides of the equation can be multiplied by $l(t)$, thus not needing to take into account the factor of $1/l(t)$ from $\frac{\partial \phi_n}{\partial X}$):

$$\begin{aligned}I_n^1\frac{\dot{X}^2}{l^2} + I_n^2\frac{\dot{l}^2}{l^2} + I_n^3\frac{2\dot{X}\dot{l}}{l^2} + I_n^4\left(\frac{2\dot{X}\dot{l}}{l^2} - \frac{\ddot{X}}{l}\right) + I_n^5\left(\frac{2\dot{l}^2}{l^2} - \frac{\ddot{l}}{l}\right) - \frac{1}{l^2}I_n^1 \\ - \frac{1}{12\kappa l^4}I_n^6 + I_n^7 + \lambda I_n^8 = \alpha\frac{\dot{X}}{l}I_n^4 + \alpha\frac{\dot{l}}{l}I_n^5 + F(t)I_n^9,\end{aligned}$$

where $I_n^k = \phi'(\theta_n)C_n^k$ for $k = 1, \ldots, 9$, with $C_n^9 = 1$, are the following functions of $\phi(\theta_n)$ and its derivatives:

$$\begin{aligned}I_n^1 &= \phi''(\theta_n)\phi'(\theta_n), \\ I_n^2 &= \phi''(\theta_n)\phi'(\theta_n)\theta_n^2, \\ I_n^3 &= \phi''(\theta_n)\phi'(\theta_n)\theta_n, \\ I_n^4 &= (\phi'(\theta_n))^2, \\ I_n^5 &= (\phi'(\theta_n))^2\theta_n,\end{aligned} \qquad \begin{aligned}I_n^6 &= \phi^{(4)}(\theta_n)\phi'(\theta_n), \\ I_n^7 &= \sin(\phi(\theta_n))\phi'(\theta_n), \\ I_n^8 &= \cos(2\phi(\theta_n))\phi'(\theta_n), \\ I_n^9 &= \phi'(\theta_n).\end{aligned}$$

Therefore, to obtain the equation for $X(t)$ all that remains is to sum over n. Since only the functions I_n^k depend on n, this can be easily done, obtaining the equation for $X(t)$:

$$\begin{aligned}I_4\frac{\ddot{X}}{l} + I_5\frac{\ddot{l}}{l} - \frac{\dot{l}^2}{l^2}(I_3 + 2I_5) - \frac{\dot{X}^2}{l^2}I_1 - \frac{2\dot{X}\dot{l}}{l^2}(I_2 + I_4) = \\ - \alpha I_5\frac{\dot{l}}{l} - \alpha I_4\frac{\dot{X}}{l} - I_6F(t) + I_7 + \lambda I_8 - \frac{1}{l^2}\left(I_1 + \frac{I_9}{12\kappa l^2}\right),\end{aligned} \tag{2.4}$$

where $I_k = \sum_n I_n^k$ for $k = 1, \ldots 9$ are the following:

$$
\begin{aligned}
I_1 &= \sum_n \phi''(\theta_n)\phi'(\theta_n), & I_6 &= \sum_n \phi'(\theta_n),\\
I_2 &= \sum_n \phi''(\theta_n)\phi'(\theta_n)\theta_n, & I_7 &= \sum_n \sin(\phi(\theta_n))\phi'(\theta_n),\\
I_3 &= \sum_n \phi''(\theta_n)\phi'(\theta_n)\theta_n^2, & I_8 &= \sum_n \cos(2\phi(\theta_n))\phi'(\theta_n),\\
I_4 &= \sum_n (\phi'(\theta_n))^2, & I_9 &= \sum_n \phi^{(4)}(\theta_n)\phi'(\theta_n). \qquad (2.5)\\
I_5 &= \sum_n (\phi'(\theta_n))^2\theta_n,
\end{aligned}
$$

We can proceed in a similar way to derive the equation for $l(t)$. First of all, we observe the relation:

$$
\begin{aligned}
\frac{\partial\phi(\theta_n)}{\partial l} &= \frac{\partial\theta_n}{\partial l}\frac{d\phi(\theta_n)}{d\theta_n},\\
&= -\frac{1}{l(t)}\theta_n\phi'(\theta_n).
\end{aligned}
$$

It is worth noting that $\frac{\partial\phi(\theta_n)}{\partial l} = \theta_n\frac{\partial\phi(\theta_n)}{\partial X}$, and consequently the equation for $l(t)$ is derived by multiplying (2.4) by θ_n:

$$
\begin{aligned}
I_n^3\frac{\dot{X}^2}{l^2} + I_n^{10}\frac{\dot{l}^2}{l^2} + I_n^2\frac{2\dot{X}\dot{l}}{l^2} + I_n^5\left(\frac{2\dot{X}\dot{l}}{l^2} - \frac{\ddot{X}}{l}\right) + I_n^{11}\left(\frac{2\dot{l}^2}{l^2} - \frac{\ddot{l}}{l}\right) - \frac{1}{l^2}I_n^3\\
- \frac{1}{12\kappa l^4}I_n^{12} + I_n^{13} + \lambda I_n^{14} = \alpha\frac{\dot{X}}{l}I_n^5 + \alpha\frac{\dot{l}}{l}I_n^{11} + F(t)I_n^{15},
\end{aligned}
$$

where I_n^k are as before for $k = 2, 3, 5$, and the following functions of ϕ_n and its derivatives for $k = 10, \ldots, 15$:

$$
\begin{aligned}
I_n^{10} &= \phi''(\theta_n)\phi'(\theta_n)\theta_n^3 = I_n^2\theta_n, & I_n^{13} &= \sin(\phi(\theta_n))\phi'(\theta_n)\theta_n = I_n^7\theta_n,\\
I_n^{11} &= (\phi'(\theta_n))^2\theta_n^2 = I_n^5\theta_n, & I_n^{14} &= \cos(2\phi(\theta_n))\phi'(\theta_n)\theta_n = I_n^8\theta_n,\\
I_n^{12} &= \phi^{(4)}(\theta_n)\phi'(\theta_n)\theta_n = I_n^9\theta_n, & I_n^{15} &= \phi'(\theta_n)\theta_n = I_n^6\theta_n.
\end{aligned}
$$

Thus, to obtain the equation for $l(t)$ all that remains is to sum over n. Since only the functions I_n^k depend on n, this can be easily done, obtaining the equation for $l(t)$:

$$I_5\frac{\ddot{X}}{l}+I_{11}\frac{\ddot{l}}{l}-\frac{\dot{l}^2}{l}(I_{10}+2I_{11})-\frac{\dot{X}^2}{l^2}I_2-\frac{2\dot{X}\dot{l}}{l^2}(I_3+I_5)= \\ -\alpha I_{11}\frac{\dot{l}}{l}-\alpha I_4\frac{\dot{X}}{l}-I_{12}F(t)+I_{13}+\lambda I_{14}-\frac{1}{l^2}\left(I_2+\frac{I_{15}}{12\kappa l^2}\right),$$

where $I_k=\sum_n I_n^k$ are the following:

$$I_2=\sum_n \phi''(\theta_n)\phi'(\theta_n)\theta_n, \qquad I_{12}=\sum_n \phi'(\theta_n)\theta_n,$$
$$I_3=\sum_n \phi''(\theta_n)\phi'(\theta_n)\theta_n^2, \qquad I_{13}=\sum_n \sin(\phi(\theta_n))\phi'(\theta_n)\theta_n,$$
$$I_4=\sum_n (\phi'(\theta_n))^2\theta_n, \qquad I_{14}=\sum_n \cos(2\phi(\theta_n))\phi'(\theta_n)\theta_n,$$
$$I_{10}=\sum_n \phi''(\theta_n)\phi'(\theta_n)\theta_n^3, \qquad I_{15}=\sum_n \phi^{(4)}(\theta_n)\phi'(\theta_n)\theta_n. \tag{2.6}$$
$$I_{11}=\sum_n (\phi'(\theta_n))^2\theta_n^2,$$

Hence, the collective coordinate equations are:

$$I_4\frac{\ddot{X}}{l}+I_5\frac{\ddot{l}}{l}-\frac{\dot{l}^2}{l^2}(I_3+2I_5)-\frac{\dot{X}^2}{l^2}I_1-\frac{2\dot{X}\dot{l}}{l^2}(I_2+I_4)= \\ -\alpha I_5\frac{\dot{l}}{l}-\alpha I_4\frac{\dot{X}}{l}-I_6F(t)+I_7+\lambda I_8-\frac{1}{l^2}\left(I_1+\frac{I_9}{12\kappa l^2}\right),$$
$$I_5\frac{\ddot{X}}{l}+I_{11}\frac{\ddot{l}}{l}-\frac{\dot{l}^2}{l}(I_{10}+2I_{11})-\frac{\dot{X}^2}{l^2}I_2-\frac{2\dot{X}\dot{l}}{l^2}(I_3+I_5)= \\ -\alpha I_{11}\frac{\dot{l}}{l}-\alpha I_5\frac{\dot{X}}{l}-I_{12}F(t)+I_{13}+\lambda I_{14}-\frac{1}{l^2}\left(I_2+\frac{I_{15}}{12\kappa l^2}\right), \tag{2.7}$$

where the I_k are as in (2.5) and (2.6).

Chapter 3

Symmetric Potential

Let us consider a potential $V(\phi_n) = -\cos(\phi_n)$. We note that this is the potential used in Section 2.2, with $\lambda = 0$. We will consider the Rice ansatz $\phi_n(t) = 4\arctan(\exp(\theta_n))$ introduced previously in Section 2.1. Since the potential that we consider in this section is symmetric, in order to have ratchet transport it is necessary to break the time symmetry by means of the force $F(t)$. With this objective, we consider a force of the form $F(t) = \epsilon(\cos(\omega t) + \cos(2\omega t))$, where ϵ is the amplitude of the force, $\omega = \frac{2\pi}{T}$ its frequency, and T its period. The aim of this section is to reproduce the results from [28]. Namely, our aim is to obtain a system of ODEs for $X(t)$ and $l(t)$ that approximates (2.1) by reproducing the calculations in [28]. The integrals calculated in this section have been evaluated symbolically using Mathematica's "Integrate" function.

3.1 Equations for the symmetric potential

First of all, we consider the system (2.7). To obtain the collective coordinate equations for $\phi_n(t)$, we need to calculate the coefficients I_k corresponding to this ansatz, and substitute them into (2.7). To do so, we will use the expressions for I_k given in (2.5) and (2.6). Hence, we first need to calculate the first, second, and fourth derivatives of ϕ with respect to θ_n:

$$\begin{aligned}\phi'(\theta_n) &= 4\frac{d}{d\theta_n}\arctan(\exp(\theta_n)),\\ &= \frac{2}{\cosh\theta_n},\\ \phi''(\theta_n) &= \frac{d}{d\theta_n}\frac{2}{\cosh\theta_n},\\ &= -\frac{2\sinh\theta_n}{\cosh^2\theta_n},\end{aligned}$$

$$\begin{aligned}\phi^{(4)}(\theta_n) &= -2\frac{d^2}{d\theta_n^2}\frac{\sinh\theta_n}{\cosh^2\theta_n},\\ &= \frac{12\sinh\theta_n}{\cosh^4\theta_n} - \frac{2\sinh\theta_n}{\cosh^2\theta_n}.\end{aligned}$$

Furthermore, for the trigonometric expressions we have $\sin\phi_n = \sin(4\arctan(\exp(\theta_n))) = -2\frac{\sinh\theta_n}{\cosh^2\theta_n} = \phi''(\theta_n)$, and $\cos(2\phi_n) = \cos(8\arctan(\exp(\theta_n))) = 1 - 8\frac{\sinh^2\theta_n}{\cosh^4\theta_n}$, which implies $I_7 = I_1$ and $I_{13} = I_2$. Therefore, we can write the I_k explicitly in terms of θ_n as the following sums:

$$\begin{aligned}I_1 &= -4\sum_n \frac{\sinh\theta_n}{\cosh^3\theta_n},\\ I_2 &= -4\sum_n \frac{\theta_n\sinh\theta_n}{\cosh^3\theta_n},\\ I_3 &= -4\sum_n \frac{\theta_n^2\sinh\theta_n}{\cosh^3\theta_n},\\ I_4 &= 4\sum_n \frac{1}{\cosh^2\theta_n},\\ I_5 &= 4\sum_n \frac{\theta_n}{\cosh^2\theta_n},\\ I_6 &= 2\sum_n \frac{1}{\cosh\theta_n},\\ I_7 &= -4\sum_n \frac{\sinh\theta_n}{\cosh^3\theta_n} = I_1,\\ I_8 &= 2\sum_n \frac{1}{\cosh\theta_n} - 16\sum_n \frac{\sinh^2\theta_n}{\cosh^5\theta_n},\\ I_9 &= 24\sum_n \frac{\sinh\theta_n}{\cosh^5\theta_n} - 4\sum_n \frac{\sinh\theta_n}{\cosh^3\theta_n},\\ I_{10} &= -4\sum_n \frac{\theta_n^3\sinh\theta_n}{\cosh^3\theta_n},\\ I_{11} &= 4\sum_n \frac{\theta_n^2}{\cosh^2\theta_n},\\ I_{12} &= 2\sum_n \frac{\theta_n}{\cosh\theta_n},\\ I_{13} &= -4\sum_n \frac{\theta_n\sinh\theta_n}{\cosh^3\theta_n} = I_2,\\ I_{14} &= 2\sum_n \frac{\theta_n}{\cosh\theta_n} - 16\sum_n \frac{\theta_n\sinh^2\theta_n}{\cosh^5\theta_n},\\ I_{15} &= 24\sum_n \frac{\theta_n\sinh\theta_n}{\cosh^5\theta_n} - 4\sum_n \frac{\theta_n\sinh\theta_n}{\cosh^3\theta_n}.\end{aligned}$$

We can see that these sums are, in general, hard to work with numerically since there is no obvious way to truncate them, as it is done with Taylor or Fourier series. Hence, in order to obtain expressions for these functions we will use the Poisson summation formula, i.e. instead of considering the sums of the form $\sum_n f(n)$, where $f(n) \equiv f(\theta_n)$ is any of the above, we consider the expansion of f as a complex Fourier series, $\sum_m \hat{f}(m) e^{2\pi i m \sqrt{\kappa} X}$, where we are taking the Fourier transform with respect to X (recall $\theta_n = \frac{n\kappa^{-1/2} - X}{l} = \frac{n - \kappa^{1/2} X}{\kappa^{1/2} l}$) [30]. Furthermore, we can rewrite the sum as a real Fourier series, which is more convenient:

$$I_j = \frac{1}{2} A_j^0 + \sum_n A_j^n \cos(2n\pi\sqrt{\kappa}X) + \sum_n B_j^n \sin(2n\pi\sqrt{\kappa}X),$$

where

$$\begin{aligned} A_j^n &= \int_{-\infty}^{\infty} f_j(\theta_n) \cos(2n\pi\sqrt{\kappa}X) dX, \\ B_j^n &= \int_{-\infty}^{\infty} f_j(\theta_n) \sin(2n\pi\sqrt{\kappa}X) dX. \end{aligned}$$

By considering these sums this way, we can obtain an expression for the I_k that we can work with by approximating them by the first non-null term (i.e. the first non-null harmonic of f).

As an example, let us consider I_1. In this case, we have $f_1(\theta_n) = \frac{\sinh(\theta_n)}{\cosh^3(\theta_n)}$. We can see that, since $\sinh x$ is an odd function and $\cosh x$ is an even function, f_1 is odd, hence we need only consider the integral of f_1 against $\sin(2\pi m\sqrt{\kappa}X)$, where $m \in \mathbb{N}$. Therefore, we have:

$$I_1 = -4 \sum_{m=1}^{\infty} B_1^m \sin(2\pi n\sqrt{\kappa}X).$$

Since we will only be considering the first non-null term, we can take $m = 1$, thus obtaining:

$$\begin{aligned} B_1^1 &= 2 \int_{-\infty}^{\infty} \frac{\sinh \frac{n\kappa^{-1/2} - X}{l}}{\cosh^3 \frac{n\kappa^{-1/2} - X}{l}} \sin(2\pi\sqrt{\kappa}X) dX, \\ &= -2\sqrt{\kappa} l \int_{-\infty}^{\infty} \frac{\sinh w}{\cosh^3 w} \sin(2\pi\sqrt{\kappa} l w) dw, \\ &= \frac{-4\pi^3 \kappa^{3/2} l^3}{\sinh(\pi^2 \sqrt{\kappa} l)}, \end{aligned}$$

and hence $I_1 \approx \frac{16\pi^3 \kappa^{3/2} l^3}{\sinh(\pi^2\sqrt{\kappa}l)} \sin(2\pi\sqrt{\kappa}X)$. We can proceed in a similar way to obtain the expressions for the remaining I_j, obtaining:

$$
\begin{aligned}
I_1 &\approx \frac{16\pi^3\kappa^{3/2}l^3}{\sinh(\pi^2\sqrt{\kappa}l)}\sin(2\pi\sqrt{\kappa}X),\\
I_2 &\approx -4\sqrt{k}l,\\
I_3 &\approx \frac{2\pi\sqrt{\kappa}l}{\sinh^3(\pi^2\sqrt{\kappa}l)}\left(2-3\kappa\pi^4l^2-(2+\kappa l^2\pi^4)\cosh(2\pi^2\sqrt{\kappa}l)+4\sqrt{\kappa}l\pi^2\sinh(2\pi^2\sqrt{\kappa}l)\right)\sin(2\pi\sqrt{\kappa}X),\\
I_4 &\approx 8\sqrt{k}l,\\
I_5 &\approx \frac{8\sqrt{\kappa}\pi l}{\sinh(\pi^2\sqrt{\kappa}l)}\left(1-\frac{\sqrt{\kappa}l\sinh(\pi^2\sqrt{\kappa}l)}{\cosh(\pi^2\sqrt{\kappa}l)}\right)\sin(2\pi\sqrt{\kappa}X),\\
I_6 &\approx 2\pi\sqrt{k}l,\\
I_7 &\approx \frac{16\pi^3\kappa^{3/2}l^3}{\sinh(\pi^2\sqrt{\kappa}l)}\sin(2\pi\sqrt{\kappa}X),\\
I_8 &\approx \frac{32\pi^3\kappa^{3/2}l^3}{3\cosh(\pi^2\sqrt{\kappa}l)}(-1+2\kappa l^2\pi^2)\cos(2\pi\sqrt{\kappa}X),\\
I_9 &\approx \frac{16\pi^3\kappa^{3/2}l^3}{\sinh(\pi^2\sqrt{\kappa}l)}(1+2\kappa l^2\pi^2)\sin(2\pi\sqrt{\kappa}X),\\
I_{10} &\approx -\pi^2\sqrt{\kappa}l,\\
I_{11} &\approx \frac{2\pi^2\sqrt{\kappa}l}{3},\\
I_{12} &\approx -\frac{2\pi^2\sqrt{\kappa}l\sinh(\pi^2\sqrt{\kappa}l)}{\cosh^2(\pi^2\sqrt{\kappa}l)}\sin(2\pi\sqrt{\kappa}X),\\
I_{13} &\approx -4\sqrt{k}l,\\
I_{14} &\approx -\frac{16\pi^2\kappa l^2}{3\cosh^2(\pi^2\sqrt{\kappa}l)}\left(2-8\kappa l^2\pi^2+\sqrt{\kappa}l\pi^2(-1+2\kappa l^2\pi^2)\frac{\sinh(\pi^2\sqrt{\kappa}l)}{\cosh(\pi^2\sqrt{\kappa}l)}\right)\sin(2\pi\sqrt{\kappa}X),\\
I_{15} &\approx -8\sqrt{\kappa}l.
\end{aligned}
$$

Hence, we can substitute these expressions for functions I_j into (2.7) to obtain the full collective coordinate equations. However, it is worth noting that, as we can see in (2.7), both of these equations have non-zero terms in the second derivatives of X and l. Therefore, it is worth looking at the relative magnitudes of the I_j to see whether or not these equations may be simplified. Up to a factor of $\sqrt{\kappa}l$, common to all the I_j, these can be seen in Fig. 3.1.

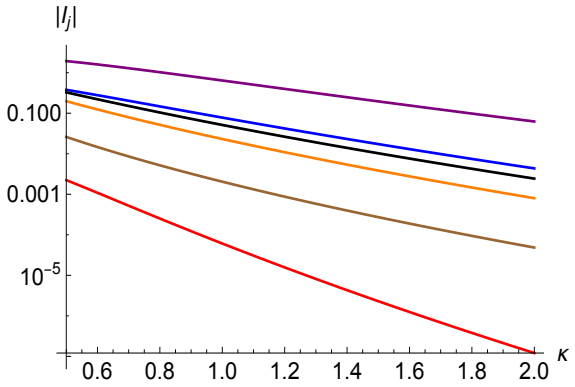

Figure 3.1: Magnitudes of $I_8, I_7, I_3, I_1, I_5, I_{12}$, and I_{14} (from top to bottom; I_3 and I_1 overlap). Since $l(t) \approx 1$, they have been evaluated at $l = 1$.

As we can see, I_5, I_{12} and I_{14} have a significantly smaller magnitude than the rest, and hence may be dropped. In particular, it is worth noting that by dropping the I_5 term, we discard the $\ddot{l}(t)$ term from the equation for X, and similarly we discard the $\ddot{X}(t)$ term from the equation for l. Thus, substituting this into (2.7) we obtain two equations with a single second order term, which is more convenient to work with, since we can in this case write the system in normal form (note however that even if we did not drop the I_5 term, we could still write the equations in normal form by adding them, multiplied by appropriate constants; dropping the I_5 term renders significantly more manageable expressions). Finally, we can normalize the ODEs by dividing the first equation in (2.7) by I_4/l, and the second one by I_{11}/l, obtaining the equations:

$$\ddot{X} + \left[J_1 \frac{\dot{l}^2}{l} - J_2 \dot{X}^2 - J_3 \right] \sin(2\pi\sqrt{\kappa}X) - \lambda J_4 \cos(2\pi\sqrt{\kappa}X) - \frac{\dot{X}\dot{l}}{l} = -\alpha\dot{X} - \frac{\pi}{4} l F(t),$$

$$\ddot{l} - \frac{\dot{l}^2}{2l} + \frac{6}{\pi^2}\frac{\dot{X}^2}{l} + J_5 \dot{X}\dot{l} \sin(2\pi\sqrt{\kappa}X) = -\alpha\dot{l} + J_6, \qquad (3.1)$$

where $J_i \equiv J_i(\kappa, l)$ are the following [28]:

$$
\begin{aligned}
J_1(\kappa,l) &= \frac{\pi\ (\cosh\left(2\sqrt{\kappa}\,l\,\pi^2\right)\ (\kappa\,l^2\,\pi^4-2)+3\,k\,l^2\,\pi^4+2)}{4\sinh^3\left(\sqrt{\kappa}\,l\,\pi^2\right)},\\
J_2(\kappa,l) &= \frac{2\,\kappa\,l\,\pi^3}{\sinh\left(\sqrt{\kappa}\,l\,\pi^2\right)},\\
J_3(\kappa,l) &= \frac{\pi^3\ (12\,\kappa\,l^2+2\,\kappa\,l^2\,\pi^2+3)}{6\,l\sinh\left(\sqrt{\kappa}\,l\,\pi^2\right)}+J_2(\kappa,l),\\
J_4(\kappa,l) &= \frac{4\,\kappa\,l^3\,\pi^3\ (2\,\kappa\,l^2\,\pi^2-1)}{3\cosh\left(\sqrt{\kappa}\,l\,\pi^2\right)},\\
J_5(\kappa,l) &= \frac{6\,\pi\,\sqrt{\kappa}\ (3\,\sqrt{\kappa}\,l\,\pi^2-2\sinh\left(2\sqrt{\kappa}\,l\,\pi^2\right)+\sqrt{\kappa}\,l\,\pi^2\cosh\left(2\sqrt{\kappa}\,l\,\pi^2\right))}{\sinh^3\left(\sqrt{\kappa}\,l\,\pi^2\right)},\\
J_6(\kappa,l) &= -\frac{12\,\kappa\,l^2\ (l^2-1)-3}{2\,\kappa\,l^3\,\pi^2}.
\end{aligned}
\tag{3.2}
$$

Finally, to perform the numerical study of this system of ODEs we need to specify some initial conditions. Since our aim is to reproduce the results in [28], we will use $X(0) = \dot{X}(0) = \dot{l}(0) = 0$, $l(0) = 1$. We will also be using the values of the constants $\alpha = \omega = 0.1$, as in [28].

3.2 Numerical study for symmetric potential

Now that we have the equations for the collective coordinates, (3.1) and (3.2), we can proceed to study the system numerically and compare the results with those obtained for the collective coordinate approximation in [28].

First of all, we can use our CC equations to estimate the so-called depinning threshold, that is the curve on the (κ, ϵ) plane that separates pinned states (i.e. no net kink motion, $\dot{X}(t) = 0$) from the region where a moving kink exists ($\dot{X}(t) \neq 0$). The results, which can be seen in Fig. 3.2, closely match the the results using the equations for the full system from [28].

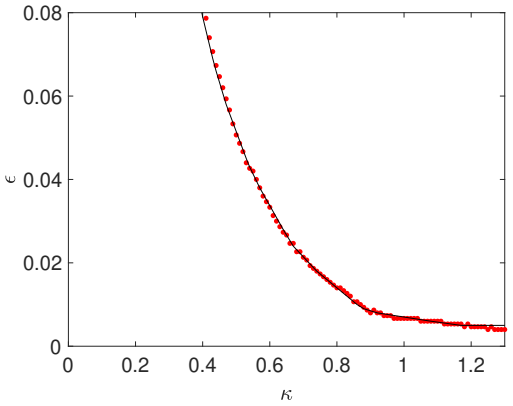

Figure 3.2: Depinning threshold for $\omega = 0.1, \alpha = 0.1$, using Collective Coordinate approximation (points in red), and equations for the full system (solid black line) [28]. Below the line no moving kink exists, above it moving kinks exist. The solid black line has been generated with data provided by Jesús Cuevas Maraver.

We have determined the threshold above which a moving kink can exist. However, there is not simply one type of motion that the system exhibits, but three: phase-locked motion, where the kink moves at constant average velocity (i.e. the velocity, when measured after each period, remains constant); chaotic or diffusive motion, where the kink moves with non-constant average velocity; and "rotating" states, where the kink does not show any net displacement after each period, but moves the same amount in each direction over one period, typically several sites of the lattice. These "rotating" states may be compared with a pendulum, in the sense that they would correspond to a pendulum rotating several times in one direction, and then back the same amount of times, so that over a single period of the force it has *on average* not moved. We can see different examples of these different motion regimes in Fig. 3.3.

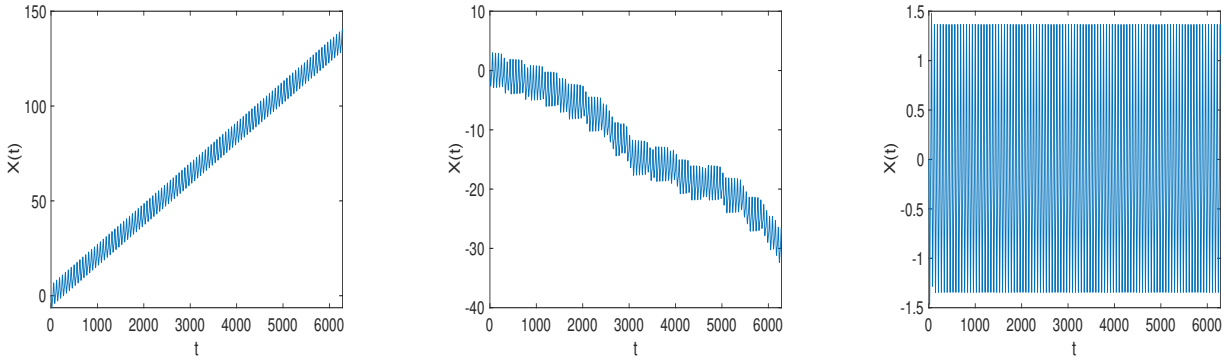

(a) (b) (c)

Figure 3.3: Examples of: (a) phase-locked motion, (b) chaotic motion, (c) rotating motion.

Computationally, we can distinguish the first two states (i.e. phase-locked and chaotic/diffusive) by calculating the position of the center of mass of the kink $X(t)$ after each period T of the force, and subsequently computing the correlation with a linear function. Additionally, if there is no net motion (i.e. the slope of the fitting function is zero), it is necessary to differentiate between rotating states and no motion. This can be done by comparing the maximum displacement of $X(t)$ over each period of the force with the lattice separation parameter $h = 1/\sqrt{\kappa}$. By proceeding this way, we can perform a detailed study on the different types of motion that the system exhibits and the regions where they appear. This can be seen in Fig. 3.4.

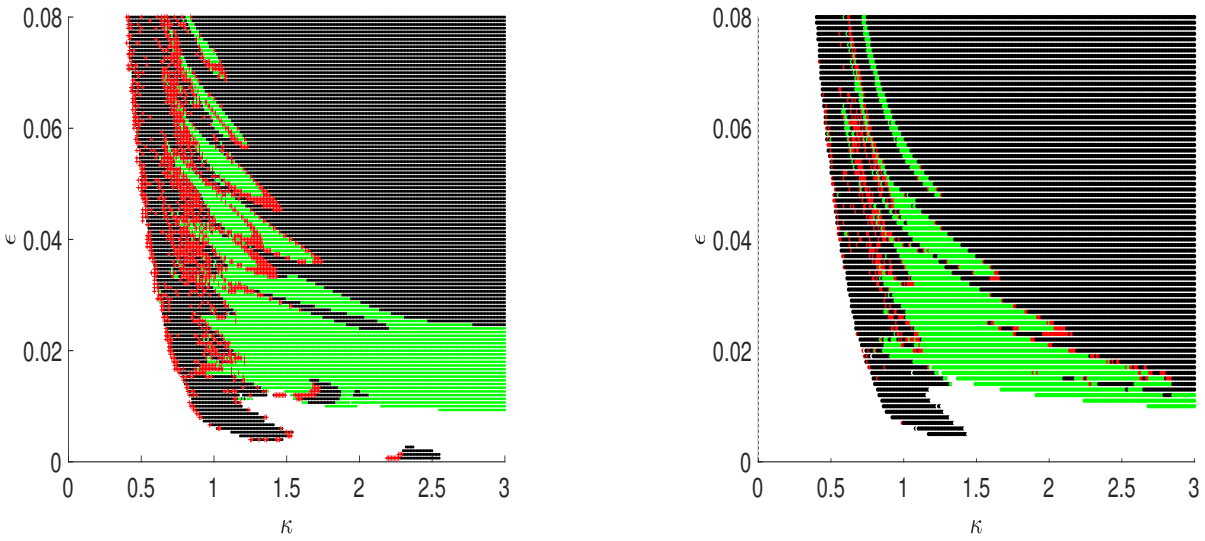

Figure 3.4: Chaotic (red), phase-locked (black), and rotating (green) transport in the (κ, ϵ) plane for (a) Collective Coordinate approximations, (b) full system [28]. Values of the parameters: $\omega = 0.1, \alpha = 0.1$. The right panel has been generated with data provided by Jesús Cuevas Maraver.

In a similar way as presented in [28], we can see that the collective coordinate approximation somewhat overestimates both the red and green regions, corresponding to chaotic and rotating motions, respectively. However, it does capture the overall pattern in the parameter plane.

Chapter 4

Asymmetric potential

We now consider a potential $V(\phi_n) = -\cos(\phi_n) + \frac{\lambda}{2}\sin(2\phi_n)$, with $\lambda \neq 0$. We observe that this potential is asymmetric, unlike the one considered before, and hence it is not necessary to break the time symmetry by means of the force $F(t)$ in order to observe ratchet transport. Therefore, we consider a slightly simpler force of the form $F(t) = \epsilon\cos(\omega t)$, where ϵ is its amplitude, $\omega = \frac{2\pi}{T}$ its frequency, and T its period. To study the dynamics of this system, we will again look at the regions on the (κ, ϵ) plane where the kink experiences the different motion regimes. Our aim is to use the equations obtained in the previous section for the symmetric potential, (3.1), and to determine whether these equations can adequately describe the system for $\lambda \neq 0$, or whether a different approach is needed, by comparing the results with the ones presented in [26] for the study of the full system of N equations. The value of λ that will be taken in this section is $\lambda = 0.46$, which is the value that was used in [26].

4.1 Numerical study for asymmetric potential using the Rice ansatz

We start by considering (3.1):

$$\ddot{X} + \left[J_1\frac{\dot{l}^2}{l} - J_2\dot{X}^2 - J_3\right]\sin(2\pi\sqrt{\kappa}X) - \lambda J_4\cos(2\pi\sqrt{\kappa}X) - \frac{\dot{X}\dot{l}}{l} = -\alpha\dot{X} - \frac{\pi}{4}lF(t),$$

$$\ddot{l} - \frac{\dot{l}^2}{2l} + \frac{6}{\pi^2}\frac{\dot{X}^2}{l} + J_5\dot{X}\dot{l}\sin(2\pi\sqrt{\kappa}X) = -\alpha\dot{l} + J_6,$$

where the J_i are as in (3.2). We can proceed as before to study the different types of motion that the system exhibits, for $0 < \epsilon < 0.1$, and $0 < \kappa < 4$. As a first step, so as to be able to better compare the results with those in [26], we will only be looking at states where there is net transport, i.e. chaotic and phase-locked states. As before, we expect to see a threshold below which no motion is observed (i.e. a depinning threshold), and above it we expect to see net motion, in particular, chaotic and phase-locked states. The results obtained using, as before, $\omega = 0.1, \alpha = 0.1$, and for $\lambda = 0.46$, can be seen in Fig. 4.1.

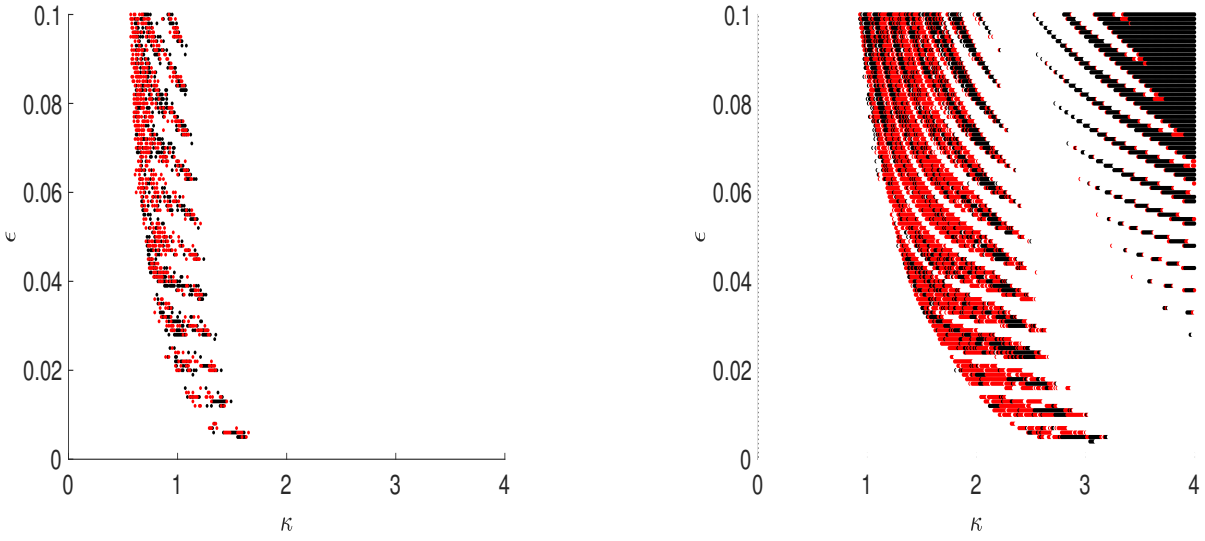

Figure 4.1: Phase-locked (blue) and chaotic (red) transport in the (κ, ϵ) plane, for (a) Collective Coordinate approximation (3.1), and (b) full system [26]. Values of the parameters: $\omega = 0.1, \alpha = 0.1$. The right panel has been generated with data provided by Jesús Cuevas Maraver.

As we can see, this does not resemble the results obtained in [26] for the full system (2.1), which we can see in Figure 4.1(b). First of all, there is kink motion for significantly lower values of both κ and ϵ. Secondly, we can see that there is no region where net transport appears for $\kappa > 2$, in stark contrast with the results for the full system (2.1). An explanation of all this can be that the ansatz used (2.2) was orginally proposed for the symmetric potential sine-Gordon equation, and hence is valid for $\lambda = 0$, but whilst the Rice ansatz approaches 0 and 2π for $x \to -\infty$ and $x \to \infty$, respectively, the double sine-Gordon's kinks approach slightly different values that depend on the minima of the potential (cf. Fig. 4.2 for a visual reference). Hence, this suggests that a different ansatz is needed to tackle this problem.

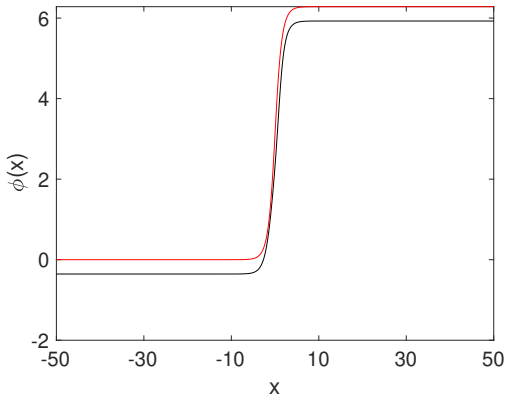

Figure 4.2: Rice ansatz (in red) for the continuous sine-Gordon equation, and ansatz for the continuous double sine-Gordon equation (in black), with $\lambda = 0.46$ [31].

4.2 New ansatz for asymmetric potential

We will now consider a different ansatz for ϕ_n that comes from the ansatz used for the continuous double sine-Gordon model in [31]. This new ansatz, which will be called QSS (Quintero-Sánchez-Salerno as in [31]) ansatz, is:

$$\phi_n \equiv \phi(\theta_n) = \phi_0 + 2\arctan\left(\frac{AB\mathrm{sgn}\lambda}{A - 1 - \eta\sinh\theta_n}\right), \tag{4.1}$$

with $\theta_n = \frac{n/\sqrt{\kappa}-X}{l}$, as before, and where $A = \sqrt{1+8\lambda^2}$, $B = \sqrt{2(4\lambda^2 - 1 + A)}$, $\eta = 2\lambda\sqrt{2(1+A)}$, and $\phi_0 = \arcsin[(1-A)/4\lambda]$, which depend only on λ. We remark that this approach, using a collective coordinate approximation directly through this ansatz, is original and that the results obtained are to be compared with those already published in [26], where authors study the discrete double sine-Gordon model in its full extent via the N-equations description.

We recall equations (2.7), the collective coordinate equations for $X(t)$ and $l(t)$:

$$\begin{aligned} I_4\frac{\ddot{X}}{l}+I_5\frac{\ddot{l}}{l}-\frac{\dot{l}^2}{l^2}(I_3+2I_5)-\frac{\dot{X}^2}{l^2}I_1-\frac{2\dot{X}\dot{l}}{l^2}(I_2+I_4)= \\ -\alpha I_5\frac{\dot{l}}{l}-\alpha I_4\frac{\dot{X}}{l}-I_6F(t)+I_7+\frac{\lambda}{2}I_8-\frac{\kappa}{l^2}\left(I_1+\frac{I_9}{12l^2}\right), \\ I_5\frac{\ddot{X}}{l}+I_{11}\frac{\ddot{l}}{l}-\frac{\dot{l}^2}{l}(I_{10}+2I_{11})-\frac{\dot{X}^2}{l^2}I_2-\frac{2\dot{X}\dot{l}}{l^2}(I_3+I_5)= \\ -\alpha I_{11}\frac{\dot{l}}{l}-\alpha I_4\frac{\dot{X}}{l}-I_{12}F(t)+I_{13}+\frac{\lambda}{2}I_{14}-\frac{\kappa}{l^2}\left(I_2+\frac{I_{15}}{12l^2}\right), \end{aligned} \tag{4.2}$$

where functions I_j are as in (2.5) and (2.6).

4.2.1 Equations for the asymmetric potential

To obtain the collective coordinate equations for the QSS ansatz, we can proceed as before, by first calculating the functions I_j corresponding to this ansatz. To do so, using (2.5) and (2.6), we will first calculate the first, second, and fourth derivatives of $\phi(\theta_n)$ with respect to θ_n:

$$\begin{aligned} \phi'(\theta_n)&=\frac{2AB\eta\cosh(\theta_n)}{A^2\left(B^2+1\right)-2(A-1)\eta\sinh(\theta_n)-2A+\eta^2\sinh^2(\theta_n)+1}, \\ \phi''(\theta_n)&=\frac{AB\eta\left(\sinh(\theta_n)\left(4A^2\left(B^2+1\right)-8A-5\eta^2+4\right)-\eta(-8A+\eta\sinh(3\theta_n)+8)\right)}{2\left(A^2\left(B^2+1\right)-2(A-1)\eta\sinh(\theta_n)-2A+\eta^2\sinh^2(\theta_n)+1\right)^2}, \\ \phi^{(4)}(\theta_n)&=\frac{P(\theta_n)}{\left(A^2\left(B^2+1\right)-2(A-1)\eta\sinh(\theta_n)-2A+\eta^2\sinh^2(\theta_n)+1\right)^4}, \end{aligned}$$

where $P(\theta_n)$ is:

$$\begin{aligned} P(\theta_n)&=2AB\eta(-9\eta^4(A^2(B^2+5)-10A+5)\sinh^5(\theta_n)+\sinh(\theta_n)((A^2(B^2+1)-2A+1)^3 \\ &\quad+34(A-1)^2\eta^4\sinh^2(2\theta_n))+8(A-1)\eta^3(A^2(3B^2+5)-10A+5)\sinh^4(\theta_n) \\ &\quad-12\eta^3\cosh^4(\theta_n)(-A+\eta\sinh(\theta_n)+1)(-2A^2B^2+2A^2-4(A-1)\eta\sinh(\theta_n)-4A+\eta^2\cosh(2\theta_n) \\ &\quad-\eta^2+2)-3\eta^2(A^4(B^4+6B^2+5)-4A^3(3B^2+5)+6A^2(B^2+5)-20A+5)\sinh^3(\theta_n) \\ &\quad+4\eta\cosh^2(\theta_n)(2A^2B^2\eta^3\sinh^3(\theta_n)+2(A-1)(A^2(B^2+1)-2A+1)^2-\eta(A^4(5B^4+6B^2+1) \\ &\quad-4A^3(3B^2+1)+6A^2(B^2+1)-4A+1)\sinh(\theta_n)-26(A-1)\eta^4\sinh^4(\theta_n)+7\eta^5\sinh^5(\theta_n)) \\ &\quad+24(A-1)\eta^5\sinh^6(\theta_n)-16(A-1)^3\eta^3\sinh^2(2\theta_n)-5\eta^6\sinh^7(\theta_n)). \end{aligned}$$

In addition to these derivatives, we also need to take into account the trigonometric functions $\sin(\phi_n)$ and $\cos(2\phi_n)$. Unfortunately, unlike before, these do not simplify nicely as to coincide with any of the derivatives above and thus lead to significantly more complex expressions for the I_j. We can write $I_k = \sum_n f_k(\theta_n)$, where the f_k are as follows:

$$f_1(\theta_n) = \frac{A^2B^2\eta^2\cosh(\theta_n)[(4-8A+4A^2(1+B^2)-5\eta^2)\sinh(\theta_n)-\eta(8-8A+\eta\sinh(3\theta_n))]}{(1-2A+A^2(1+B^2)-2(A-1)\eta\sinh(\theta_n)+\eta^2\sinh^2(\theta_n))^3},$$

$$f_2(\theta_n) = \frac{\theta_n A^2B^2\eta^2\cosh(\theta_n)[(4-8A+4A^2(1+B^2)-5\eta^2)\sinh(\theta_n)-\eta(8-8A+\eta\sinh(3\theta_n))]}{(1-2A+A^2(1+B^2)-2(A-1)\eta\sinh(\theta_n)+\eta^2\sinh^2(\theta_n))^3},$$

$$f_3(\theta_n) = \frac{\theta_n^2 A^2B^2\eta^2\cosh(\theta_n)[(4-8A+4A^2(1+B^2)-5\eta^2)\sinh(\theta_n)-\eta(8-8A+\eta\sinh(3\theta_n))]}{(1-2A+A^2(1+B^2)-2(A-1)\eta\sinh(\theta_n)+\eta^2\sinh^2(\theta_n))^3},$$

$$f_4(\theta_n) = \frac{4A^2B^2\eta^2\cosh^2(\theta_n)}{(A(AB^2+A-2)+\eta\sinh(\theta_n)(-2A+\eta\sinh(\theta_n)+2)+1)^2},$$

$$f_5(\theta_n) = \frac{4A^2B^2\theta_n\eta^2\cosh^2(\theta_n)}{(A(AB^2+A-2)+\eta\sinh(\theta_n)(-2A+\eta\sinh(\theta_n)+2)+1)^2},$$

$$f_6(\theta_n) = \frac{2AB\eta\cosh(\theta_n)}{A^2(B^2+1)-2(A-1)\eta\sinh(\theta_n)-2A+\eta^2\sinh^2(\theta_n)+1},$$

$$f_7(\theta_n) = \frac{2AB\eta\cosh(\theta_n)\sin(\phi_n)}{A^2(B^2+1)-2(A-1)\eta\sinh(\theta_n)-2A+\eta^2\sinh^2(\theta_n)+1},$$

$$f_8(\theta_n) = \frac{2AB\eta\cosh(\theta_n)\cos(2\phi_n)}{A^2(B^2+1)-2(A-1)\eta\sinh(\theta_n)-2A+\eta^2\sinh^2(\theta_n)+1},$$

$$f_9(\theta_n) = \frac{2AB\eta\cosh(\theta_n)P}{(A^2(B^2+1)-2(A-1)\eta\sinh(\theta_n)-2A+\eta^2\sinh^2(\theta_n)+1)^5},$$

$$f_{10}(\theta_n) = \frac{\theta_n^3 A^2B^2\eta^2\cosh(\theta_n)[(4-8A+4A^2(1+B^2)-5\eta^2)\sinh(\theta_n)-\eta(8-8A+\eta\sinh(3\theta_n))]}{(1-2A+A^2(1+B^2)-2(A-1)\eta\sinh(\theta_n)+\eta^2\sinh^2(\theta_n))^3},$$

$$f_{11}(\theta_n) = \frac{4A^2B^2\theta_n^2\eta^2\cosh^2(\theta_n)}{(A(AB^2+A-2)+\eta\sinh(\theta_n)(-2A+\eta\sinh(\theta_n)+2)+1)^2},$$

$$f_{12}(\theta_n) = \frac{2\theta_n AB\eta\cosh(\theta_n)}{A^2(B^2+1)-2(A-1)\eta\sinh(\theta_n)-2A+\eta^2\sinh^2(\theta_n)+1},$$

$$f_{13}(\theta_n) = \frac{2\theta_n AB\eta\cosh(\theta_n)\sin(\phi_n)}{A^2(B^2+1)-2(A-1)\eta\sinh(\theta_n)-2A+\eta^2\sinh^2(\theta_n)+1},$$

$$f_{14}(\theta_n) = \frac{2\theta_n AB\eta\cosh(\theta_n)\cos(2\phi_n)}{A^2(B^2+1)-2(A-1)\eta\sinh(\theta_n)-2A+\eta^2\sinh^2(\theta_n)+1},$$

$$f_{15}(\theta_n) = \frac{2\theta_n AB\eta\cosh(\theta_n)P}{(A^2(B^2+1)-2(A-1)\eta\sinh(\theta_n)-2A+\eta^2\sinh^2(\theta_n)+1)^5}$$

As was the case with the symmetric potential, these sums are difficult to work with numerically, since there is no obvious way to truncate them. Hence, in order to obtain usable expressions for these coefficients we will proceed as before, using the Poisson summation formula. Therefore, since $I_j = \sum_n f_j(n)$, we need to calculate the Fourier transforms of each f_j. As before, this is a Fourier series, and hence it is convenient to write:

$$I_j = \frac{1}{2}A_j^0 + \sum_n A_j^n \cos(2n\pi\sqrt{\kappa}X) + \sum_n B_j^n \sin(2n\pi\sqrt{\kappa}X),$$

where:

$$A_j^n = \int_{-\infty}^{\infty} f_j(\theta_n)\cos(2n\pi\sqrt{\kappa}X)dX,$$
$$B_j^n = \int_{-\infty}^{\infty} f_j(\theta_n)\sin(2n\pi\sqrt{\kappa}X)dX.$$

Let us start by calculating the first function, I_1. First of all, the first (constant) term of the series is considered, which we will denote by A_0^1. Up to a factor $\sqrt{\kappa}l$, common to all the I_j which can then be cancelled out in (4.2), we obtain:

$$\begin{aligned} A_0^1 &= \int_{-\infty}^{\infty} \frac{A^2B^2\eta^2\cosh x[(4-8A+4A^2(1+B^2)-5\eta^2)\sinh x - \eta(8-8A+\eta\sinh 3x)]}{(1-2A+A^2(1+B^2)-2(A-1)\eta\sinh x+\eta^2\sinh^2 x)^3}dx \\ &= 0. \end{aligned}$$

As we can see, this integral vanishes, and hence we need to consider the first order terms in the Fourier series, A_1^1 and B_1^1. It is worth mentioning that this integral has been calculated numerically using Mathematica's "NIntegrate" function to a value of 0; however, the integrand is not symmetric nor periodic to be able to assert its value beyond machine precision. The values of both A_1^1 and B_1^1 will depend on the values of both κ and $l(t)$, and in particular on the value of the product $\sqrt{\kappa}l$. This in particular means that, since these integrals have no closed form, it would in theory be necessary to calculate each of these integrals at each step of the numerical resolution of system (4.2) since $l(t)$ is one of the two variables, which is unfeasible. However, it is possible to instead calculate an interpolant surface which may allow for the evaluation of the integrals over the range where κ and $l(t)$ lie. This interpolant can be computed at reasonable speed by software such as Mathematica, yielding functions that are manageable to deal with for the numerical resolution of the problem. Since we are varying κ from 0.1 ($\kappa = 0$ is a singularity, and it is noted that for $\kappa \leq 0.1$ and $\epsilon \leq 0.1$ no moving kink exists) to 4, the range of interpolation taken was $0.1 \leq \kappa \leq 4$, and $0.01 \leq l \leq 2$.

We can repeat this process to obtain expressions for the I_j in terms of their first non-null harmonic (for simplicity, we will use A_j^n and B_j^n for the non-constant coefficients instead of

the full integral expression; for those functions that are approximated by a constant, the value of this constant obtained via numerical integration is provided, for $\lambda = 0.46$):

$$
\begin{aligned}
I_1 &\approx A_1^1(\kappa, l)\cos(2\pi\sqrt{\kappa}X) + B_1^1(\kappa, l)\sin(2\pi\sqrt{\kappa}X),\\
I_2 &\approx -3.40878,\\
I_3 &\approx -2.09823,\\
I_4 &\approx 6.81756,\\
I_5 &\approx 2.09823,\\
I_6 &\approx 2\pi,\\
I_7 &\approx A_7^1(\kappa, l)\cos(2\pi\sqrt{\kappa}X) + B_7^1(\kappa, l)\sin(2\pi\sqrt{\kappa}X),\\
I_8 &\approx A_8^1(\kappa, l)\cos(2\pi\sqrt{\kappa}X) + B_8^1(\kappa, l)\sin(2\pi\sqrt{\kappa}X),\\
I_9 &\approx A_9^1(\kappa, l)\cos(2\pi\sqrt{\kappa}X) + B_9^1(\kappa, l)\sin(2\pi\sqrt{\kappa}X),\\
I_{10} &\approx -13.7068,\\
I_{11} &\approx 9.13786,\\
I_{12} &\approx 1.08865,\\
I_{13} &\approx -4.33394,\\
I_{14} &\approx -1.97697,\\
I_{15} &\approx 2.47729,
\end{aligned}
$$

As we can see, some of the I_j depend explicitly on both κ and l (in particular, on the product $\sqrt{\kappa}l$). However, this is not the case for most of the coefficients, which can be approximated by the constant term with no explicit dependence on κ or l; since λ is a fixed parameter, these will be constant throughout our simulations. For those coefficients whose constant term does vanish (namely I_1, I_7, I_8, I_9), to find the coefficients for the first harmonic we need to proceed in an analogous way as for I_1 described above, namely constructing an interpolant over the same domain of κ and $l(t)$.

Once we have calculated these interpolants, in order to determine whether one of these coefficients is small enough to be neglected in (4.2), as was the case for the symmetric potential, we can plot their amplitudes in terms of the product $\sqrt{\kappa}l$ (this was done by fixing l to one and varying κ; their amplitude was taken to be the usual L^2 norm). This can be seen in Fig. 4.3. In particular, from this figure we see that they are significant for values of small enough values of $\sqrt{\kappa}l$, hence must be taken into account in (4.2).

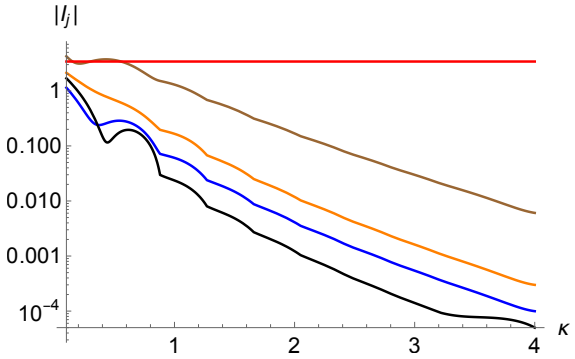

Figure 4.3: Amplitudes of the coefficients I_1, I_7, I_8, I_9 (blue, black, orange, brown respectively) vs κ compared with I_2 (red) for $0 < \kappa \leq 4$ ($\kappa = 0$ is a singularity).

Having determined the coefficients for (4.2), we perform the simulations to determine the different types of motion the system exhibits in terms of the discretization parameter κ and the amplitude of the force, ϵ. In particular, as was the case for the Rice ansatz, we expect to see three different types of motion, in addition to the stationary state: phase-locked motion, chaotic motion, and rotating states. To differentiate between the different types of motions we can proceed as before. Namely, we first calculate $X(t)$ after each period of the force, and then we fit these points by a linear function. If the slope of this function is different to zero, then we have a phase-locked state if the fit is good (that is, if the R^2 coefficient is close to 1), and chaotic otherwise. If this slope is close to 0, then to distinguish between stationary and rotating states we compare the maximum displacement of $X(t)$ over each period of the force with the lattice separation parameter $h = 1/\sqrt{\kappa}$.

The results obtained can be seen in Fig. 4.4. The initial conditions taken are $X(0) = \dot{X}(0) = \dot{l}(0) = 0$, $l(0) = 0.8$ (average value of the width observed for $\lambda = 0.46$; as shown in [26], the results should not depend on the initial conditions chosen, although the closer these are to the final state the faster the stationary solution will be obtained and hence the lower the computational time needed will be).

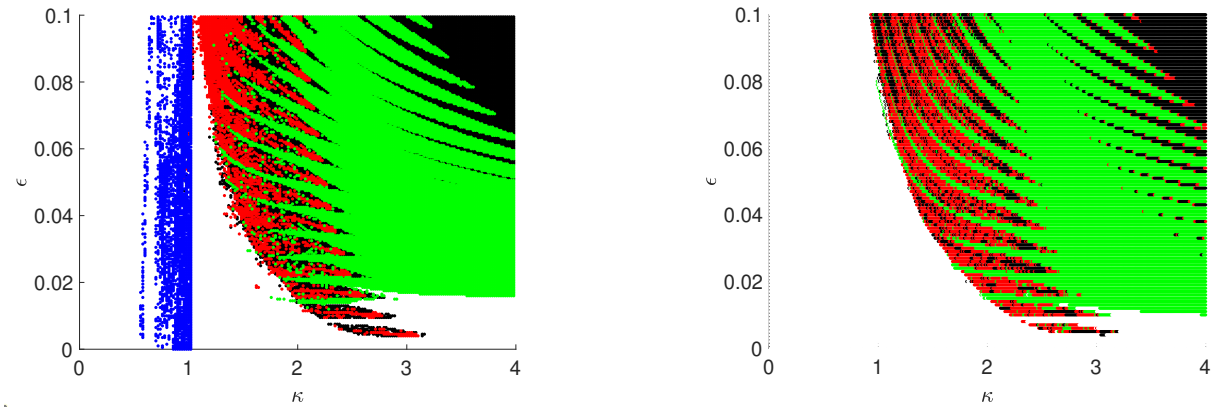

(a) (b)

Figure 4.4: Different types of motion of the kink, in terms of the discretization parameter κ and the amplitude of the force ϵ, using (a) collective coordinate approximation, (b) full system (2.1) [26]. White area: No net motion; black area: phase-locked motion; red area: chaotic motion; green area: rotating states; blue area: solutions blow up. Values of the parameters: $\omega = 0.1, \alpha = 0.1, \lambda = 0.46$. The right panel has been generated with data provided by Jesús Cuevas Maraver.

We can see that the results obtained are close to the results from the simulation of the full system; in particular, the region at $\kappa > 3$ with net kink motion, that was not reproduced with Rice ansatz, is now reproduced. There are however two differences worth mentioning. First, the rotating states region (i.e. the green region in 4.4) is slightly overestimated in the collective coordinate approximation, as is the phase-locked states region (i.e. the black region in 4.4). Nevertheless, this approximation satisfactorily captures the general behaviour of the system. Secondly, and more relevantly, it is worth noting that there is a small vertical line at $\kappa \approx 1$ where some points (i.e. net kink motion) appear; however, this is not due to any actual net kink motion, but to the solutions of the system "blowing up" at some points for $\kappa \lesssim 1$. These are the points represented in blue. This suggests that the Collective Coordinate approximation made might not be valid on this region. However, a possible explanation for this is related to the way we approximated the $\phi_{n\pm1}$ in the expression for the discrete Laplacian. We recall that we approximated them via their Taylor expansion around $\delta = 0$, where $\delta = 1/(\sqrt{\kappa}l)$, up to fourth order, i.e.:

$$\phi(\theta_n \pm \delta) \approx \phi(\theta_n) \pm \phi'(\theta_n)\delta + \frac{1}{2}\phi''(\theta_n)\delta^2 \pm \frac{1}{3!}\phi^{(3)}(\theta_n)\delta^3 + \frac{1}{4!}\phi^{(4)}(\theta_n)\delta^4.$$

This approximation is valid for values of δ sufficiently small, i.e. κ sufficiently large (in this case it is valid for the region of interest, $\kappa \gtrsim 1$). In particular, for small values of κ, the terms

in the higher order even derivatives (recall that we are adding $\phi(\theta_n + \delta) + \phi(\theta_n - \delta) - 2\phi(\theta_n)$, hence the odd order terms, as well as the zeroth order one, cancel out) will be significant and hence should be taken into account. However, since we are interested in studying the region where there is net kink motion, this region where $\kappa \lesssim 1$ need not be taken into account. In fact, for $\sqrt{\kappa} l \gtrsim 1$, the fourth order term may be dropped, and we expect the number of terms needed for the approximation to be good to grow very quickly for $\sqrt{\kappa} l \leq 1$.

Chapter 5

Conclusions and Perspectives

For the first part of this project, the forced and damped discrete sine-Gordon system (hereafter referred to as the symmetric potential system) was considered. The aim in this first part was to reproduce the results given in [28]. First of all, a collective coordinate (CC) approach was taken so as to reduce the system from a (possibly) large number N of ODEs to just two. This was done by means of the so-called Generalized Travelling Wave method, with the resulting equations being used for the numerical simulations. Overall, the results obtained largely agree with those obtained in [28].

Once the CC equations for the symmetric potential system were obtained, an attempt was made to extend them to the study of the damped and forced double sine-Gordon system (hereafter referred to as the asymmetric potential system). This attempt ultimately proved unsuccessful, owing to the extra harmonic term in the potential rendering the previously used ansatz incorrect. For the study of the system in more detail however, a different ansatz was proposed and the CC equations corresponding to this ansatz were derived. Once the resulting system of two coupled second-order ODEs was obtained, numerical simulations of it were ran and compared with the results using the full N equation system. Unlike before, the results obtained this time agreed reasonably well with those obtained in [26] for the full system. The results obtained in this part of the project are original and, together with some extension to the study of the stability of the different orbits that appear, might be worthy of publication.

Overall, the main goal of obtaining a collective coordinate approximation of the damped and forced discrete double sine-Gordon system was achieved, providing a reasonable and time efficient approximation of the system of N equations. However, the fact that the approximation did not provide good results for $\kappa \lesssim 1$, even though it did not pose any problems in our case, could be problematic when considering other values of the parameters, and in such

case it might be necessary to use higher order terms in the approximation of the discrete Laplacian.

Finally, as an extension of this project, it could be interesting to study the stability of the periodic and travelling wave solutions, using Floquet analysis, with the aid of the Collective Coordinate equations. To do so, the variational equations would need to be calculated, which would most certainly imply making further approximations [32, 33]. As for the chaotic orbits, which may not be studied using Floquet analysis, the variational equations can be used to calculate the associated Lyapunov exponents [32, 34]. Even though this study would require further approximations, if successful these would provide, in a similar way as the approximations made in this project, a computationally effective way of determining the stability of solutions when compared to the full system of N coupled equations. In addition to this study of the stability, it could be worth extending the study of the ratchet phenomenon with collective coordinate approximations to a ϕ^4 potential (that is a potential of the form $\phi^2/2 - \phi^4/4$ instead of the periodic one used here), where the ratchet behaviour of kinks has been studied in the continuous case [35, 36]. In addition to changing the potential, studying the system under other types of forces, such as parametric forces that depend on the field ϕ – that is, $\phi_n \equiv \phi(\theta_n)$ in the discrete case – as well as on time could also present an interesting extension. For these parametric forces the ratchet phenomenon and the existence of kinks has been studied, in the continuous case, both for the sine-Gordon [37, 38] and the ϕ^4 potential [37, 39].

Bibliography

[1] Cuevas-Maraver, Jesús & Kevrekidis, Panayotis & Williams, Floyd. (2014). *The sine-Gordon Model and its Applications: From Pendula and Josephson Junctions to Gravity and High-Energy Physics.* (Springer International Publishing Switzerland). https://doi.org/doi/10.1007/978-3-319-06722-3.

[2] Scott, A.C. (1969). *A Nonlinear Klein-Gordon Equation.* American Journal of Physics 37, 52. https://doi.org/10.1119/1.1975404.

[3] Voglis, N. (2003). *Solitons and breathers from the third integral of motion in galaxies.* Monthly Notices of the Royal Astronomical Society. 344. 575 - 582. https://doi.org/10.1046/j.1365-8711.2003.06848.x.

[4] Li, Y. & Lu, X. & Hou, C. *The Sine-Gordon solitons in nematic liquid crystals under the external electric field.* Results in Physics, Volume 10. https://doi.org/10.1016/j.rinp.2018.06.012.

[5] Braun, Oleg & Kivshar, Yuri. (1998). *Nonlinear dynamics of the Frenkel-Kontorova model.* Physics Reports, Volume 306, Issues 1–2. https://doi.org/10.1016/S0370-1573(98)00029-5.

[6] Watanabe, S. & van der Zant, H.S.J. & Strogatz, S.H. & Orlando, T.P. (1996). *Dynamics of circular arrays of Josephson junctions and the discrete sine-Gordon equation.* Physica D: Nonlinear Phenomena, Volume 97, Issue 4. https://doi.org/10.1016/0167-2789(96)00083-8.

[7] Englander, S.W. & Kallenbach, N.R. & Heeger, N.R. & Krumhansl, J.A. & Litwin, S. (1980). *Nature of the open state in long polynucleotide double helices: possibility of soliton excitations.* Proceedings of the National Academy of Sciences 7222-7226. doi:10.1073/pnas.77.12.7222.

[8] Salerno, Mario. (1985). *A mechanical analog for the double sine-Gordon equation.* Physica D: Nonlinear Phenomena, Volume 17, Issue 2. https://doi.org/10.1016/0167-2789(85)90007-7.

[9] Reimann, Peter. (2002). *Brownian Motors: Noisy Transport Far From Equilibrium.* Phys. Rep. 361. https://doi.org/10.1016/S0370-1573(01)00081-3.

[10] Hanggi, Peter & Marchesoni, Fabio. (2008). *Artificial Brownian motors: Controlling transport on the nanoscale.* Review of Modern Physics. 81. https://doi.org/10.1103/RevModPhys.81.387.

[11] Flach, S. & Yevtushenko, O. & Zolotaryuk, Y. (2000). *Directed Current due to Broken Time-Space Symmetry.* Physical Review Letters 84.2358. https://doi.org/10.1103/PhysRevLett.84.2358

[12] Reimann, Peter. (2001). *Supersymmetric Ratchets.* Physical Review Letters 86. 4992-5. https://doi.org/10.1103/PhysRevLett.86.4992.

[13] Salerno, Mario & Zolotaryuk, Yaroslav. (2002). *Soliton ratchetlike dynamics by ac forces with harmonic mixing.* Physical Review E 65.056603. https://doi.org/10.1103/PhysRevE.65.056603.

[14] Falo, F. & Martínez, P. & Mazo, J. et al. (2002). *Fluxon ratchet potentials in superconducting circuits.* Applied Physics A 75, 263–269. https://doi.org/10.1007/s003390201325.

[15] Ustinov, AV & Coqui, C & Kemp, Alexander & Zolotaryuk, Yaroslav & Salerno, Mario. (2004). *Ratchetlike Dynamics of Fluxons in Annular Josephson Junctions Driven by Biharmonic Microwave Fields.* Physical Review Letters 93. 087001. https://doi.org/10.1103/PhysRevLett.93.087001.

[16] Beck, M. & Goldobin, E. & Neuhaus, M. & Siegel, M. & Kleiner, R. & Koelle, D. (2005). *High-Efficiency Deterministic Josephson Vortex Ratchet.* Physical Review Letters 95.090603. https://doi.org/10.1103/PhysRevLett.95.090603.

[17] Ooi, S. & Savel'ev, S. & Gaifullin, Marat & Mochiku, T & Hirata, Kazuto & Nori, Franco. (2007). *Nonlinear Nanodevices Using Magnetic Flux Quanta.* Physical Review Letters 99. 207003. https://doi.org/10.1103/PhysRevLett.99.207003.

[18] Salger, Tobias & Kling, Sebastian & Hecking, Tim & Geckeler, Carsten & Morales-Molina, Luis & Weitz, Martin. (2009). *Directed Transport of Atoms in a Hamiltonian Quantum Ratchet.* Science 326. 1241-3. https://doi.org/10.1126/science.1179546.

[19] Ajdari, A. & Mukamel, D. & Peliti, L. & Prost, J. (1994). *Rectified motion induced by AC forces in periodic structures.* J. Phys. I 4, 1551-1561. doi:10.1051/jp1:1994206

[20] Dante R. Chialvo & Mark M. Millonas. (1995). *Asymmetric unbiased fluctuations are sufficient for the operation of a correlation ratchet.* Physics Letters A, Volume 209, Issues 1–2. https://doi.org/10.1016/0375-9601(95)00773-0.

[21] Cole, D. & Bending, S. & Savel'ev, S. et al. (2006). *Ratchet without spatial asymmetry for controlling the motion of magnetic flux quanta using time-asymmetric drives.* Nature Mater 5, 305–311. https://doi.org/10.1038/nmat1608

[22] Feynman, Richard & Leighton, Robert & Sands, Mark. (1965). *The Feyman Lectures on Physics, Volume I.* Addison-Wesley. https://doi.org/10.1063/1.3051743.

[23] Kay ER & Leigh DA & Zerbetto F. (2007)*Synthetic molecular motors and mechanical machines.* Angew Chem Int Ed Engl. 46(1-2):72-191. https://doi.org/10.1002/anie.200504313.

[24] Cartwright, J. H. E. & Checa, A. G. & Rousseau, M. (2013) *Pearls Are Self-Organized Natural Ratchets.* 29 (26), 8370-8376 https://doi.org/10.1021/la4014202.

[25] Schneider, W. & Seeger, K. (1966). *Harmonic mixing of microwaves by warm electrons in germanium* Applied Physics Letters 8, 133. https://doi.org/10.1063/1.1754521.

[26] Cuevas-Maraver, Jesús & Sánchez-Rey, Bernardo & Salerno, Mario. (2010). *Regular and chaotic transport of discrete solitons in asymmetric potentials.* Physical review. E, Statistical, nonlinear, and soft matter physics. 82. 016604. https://doi.org/10.1103/PhysRevE.82.016604.

[27] Mertens, Franz & Schnitzer, H. & Bishop, Ar. (1997). *Hierarchy of Equations of Motion for Nonlinear Coherent Excitations Applied to Magnetic Vortices.* Physical Review B 56. 2510. https://doi.org/10.1103/PhysRevB.56.2510.

[28] Sánchez-Rey, Bernardo & Quintero, Niurka & Cuevas-Maraver, Jesús & Alejo, Miguel. (2014). *Collective Coordinates Theory for Discrete Soliton Ratchets in the sine-Gordon Model.* Physical review. E, Statistical, nonlinear, and soft matter physics. 90. 042922. https://doi.org/10.1103/PhysRevE.90.042922.

[29] Salerno, M. & Scott, A. (1982) *Linewidth for fluxon oscillators.* Physical Review B 26. 2474. https://doi.org/doi/10.1103/PhysRevB.26.2474.

[30] Deitmar, A. & Echterhoff, S. (2014). *Principles of Harmonic Analysis.* Springer International Publishing. https://link.springer.com/book/10.1007/978-3-319-05792-7

[31] Quintero, Niurka & Sánchez-Rey, Bernardo & Salerno, Mario. (2005). *Analytical approach to soliton ratchets in asymmetric potentials.* Physical review E, Statistical, nonlinear, and soft matter physics. 72. 016610. https://doi.org/10.1103/PhysRevE.72.016610.

[32] Parker, T.S. & Chua, L.O. (1989). *Practical Numerical Algorithms for Chaotic Systems.* Springer New York, NY. https://doi.org/10.1007/978-1-4612-3486-9.

[33] Skubachevskii, Alexander & Walther, Hans-Otto. (2006). *On the Floquet Multipliers of Periodic Solutions to Non-linear Functional Differential Equations.* Journal of Dynamics and Differential Equations. 18. 257-355. https://doi.org/10.1007/s10884-006-9006-5.

[34] Balcerzak, Marek & Pikunov, Danylo & Dabrowski, Artur. (2018). *The fastest, simplified method of Lyapunov exponents spectrum estimation for continuous-time dynamical systems.* Nonlinear Dynamics. 94. https://doi.org/10.1007/s11071-018-4544-z.

[35] Kevrekidis, Panayotis & Cuevas-Maraver, Jesús. (2019). *A Dynamical Perspective on the ϕ^4 Model: Past, Present and Future.* Nonlinear Systems and Complexity. https://doi.org/10.1007/978-3-030-11839-6.

[36] Morales-Molina, Luis & Mertens, Franz & Sánchez, Angel. (2005). *Ratchet behavior in nonlinear Klein-Gordon systems with pointlike inhomogeneities.* Physical Review E 72, 016612. https://doi.org/10.1103/PhysRevE.72.016612.

[37] Zamora-Sillero, Elías & Quintero, Niurka & Mertens, Franz. (2006). *Ratchet effect in a damped sine-Gordon system with additive and parametric ac driving forces.* Physical review. E, Statistical, nonlinear, and soft matter physics. 74. 046607. https://doi.org/10.1103/PhysRevE.74.046607.

[38] Costantini, Giulio & Marchesoni, Fabio & Borromeo, M. (2002). *String ratchets: Ac driven asymmetric kinks.* Physical review. E, Statistical, nonlinear, and soft matter physics. 65. 051103. https://doi.org/10.1103/PhysRevE.65.051103.

[39] Kivshar, Yuri S. & Sánchez, Angel & Vázquez, Luis. (1992). *Kink decay in a parametrically driven φ^4 chain.* Physical Review A 45.1207. https://doi.org/10.1103/PhysRevA.45.1207.

Appendix A

Codes

Below is the Mathematica code used to simulate the Collective Coordinate equations and produce Figure 4.4(a).

```
(*Values of the parameters*)
lambda = 0.46;
w = 0.1;
T = 2 Pi/w;
alpha = 0.1;

(*Values of constants in ansatz*)
A = Sqrt[1+8 lambda^2];
eta = 2 lambda Sqrt[2 (1+A)];
B = Sqrt[2 (4 lambda^2-1+A)];
phi0 = ArcSin[(1-A)/(4 lambda)];
ansatz[x_] := phi0 + 2 ArcTan[A B/(A-1-eta Sinh[x])];

(*We calculate the derivatives of the ansatz*)

deriv1[x_]:=ansatz'[x];
deriv2[x_]:=ansatz''[x];
deriv4[x_]:=ansatz''''[x];
trig1[x_] := Sin[ansatz[x]];
trig2[x_] := Cos[2 ansatz[x]];

(*We calculate the f_k corresponding to each of the I_k*)

I1[x_]:=Simplify[deriv1[x] deriv2[x]];
```

```
I2[x_]:=Simplify[deriv1[x] deriv2[x] x];
I3[x_]:=Simplify[deriv1[x] deriv2[x] x^2];
I4[x_]:=Simplify[deriv1[x]^2];
I5[x_]:=Simplify[deriv1[x]^2 x ];
I6[x_]:=Simplify[deriv1[x]];
I7[x_]:=Simplify[deriv1[x] trig1[x]];
I8[x_]:=Simplify[deriv1[x]trig2[x]];
I9[x_]:=Simplify[deriv1[x] deriv4[x]];
I10[x_]:=Simplify[deriv1[x] deriv2[x] x^3];
I11[x_]:=Simplify[deriv1[x]^2 x^2];
I12[x_]:=Simplify[deriv1[x] x];
I13[x_]:=Simplify[deriv1[x] trig1[x] x];
I14[x_]:=Simplify[deriv1[x]trig2[x] x];
I15[x_]:=Simplify[deriv1[x] deriv4[x] x];

(*We interpolate the non-constant coefficients over the region of interest*)

h1=FunctionInterpolation[NIntegrate[Simplify[I1[x] Cos[2 Pi Sqrt[k] l
    x]],{x,-Infinity,Infinity}],{k,0.1,4},{l,0.01,2}];
h7=FunctionInterpolation[NIntegrate[Simplify[I7[x] Cos[2 Pi Sqrt[k] l
    x]],{x,-Infinity,Infinity}],{k,0.1,4},{l,0.01,2}];
h8=FunctionInterpolation[NIntegrate[Simplify[I8[x] Cos[2 Pi Sqrt[k] l
    x]],{x,-Infinity,Infinity}],{k,0.1,4},{l,0.01,2}];
h9=FunctionInterpolation[NIntegrate[Simplify[I9[x] Cos[2 Pi Sqrt[k] l
    x]],{x,-Infinity,Infinity}],{k,0.1,4},{l,0.01,2}];
h16=FunctionInterpolation[-NIntegrate[Simplify[I1[x] Sin[2 Pi Sqrt[k] l
    x]],{x,-Infinity,Infinity}],{k,0.1,4},{l,0.01,2}];
h17=FunctionInterpolation[-NIntegrate[Simplify[I7[x] Sin[2 Pi Sqrt[k] l
    x]],{x,-Infinity,Infinity}],{k,0.1,4},{l,0.01,2}];
h18=FunctionInterpolation[-NIntegrate[Simplify[I8[x] Sin[2 Pi Sqrt[k] l
    x]],{x,-Infinity,Infinity}],{k,0.1,4},{l,0.01,2}];
h19=FunctionInterpolation[-NIntegrate[Simplify[I9[x] Sin[2 Pi Sqrt[k] l
    x]],{x,-Infinity,Infinity}],{k,0.1,4},{l,0.01,2}];
f1[a_,b_]:=h1[a,b];
f7[a_,b_]:=h7[a,b];
f8[a_,b_]:=h8[a,b];
f9[a_,b_]:=h9[a,b];
f16[a_,b_]:=h16[a,b];
f17[a_,b_]:=h17[a,b];
f18[a_,b_]:=h18[a,b];
f19[a_,b_]:=h19[a,b];

(*We calculate the remaining (constant) coefficients, and define functions I_k*)
```

```
J2=NIntegrate[I2[x],{x,-Infinity,Infinity}];
J3=NIntegrate[I3[x],{x,-Infinity,Infinity}];
J4=NIntegrate[I4[x],{x,-Infinity,Infinity}];
J5=NIntegrate[I5[x],{x,-Infinity,Infinity}];
J6=NIntegrate[I6[x],{x,-Infinity,Infinity}];
J10=NIntegrate[I10[x],{x,-Infinity,Infinity}];
J11=NIntegrate[I11[x],{x,-Infinity,Infinity}];
J12=NIntegrate[I12[x],{x,-Infinity,Infinity}];
J13=NIntegrate[I13[x],{x,-Infinity,Infinity}];
J14=NIntegrate[I14[x],{x,-Infinity,Infinity}];
J15=NIntegrate[I15[x],{x,-Infinity,Infinity}];

P1[k_,l_]:=2 Sqrt[k] l f16[k,l] Sin[2 Pi Sqrt[k] u[t]]+2 Sqrt[k] l f1[k,l] Cos[2
   Pi Sqrt[k] u[t]];
P2[k_,l_]:=Sqrt[k] l J2;
P3[k_,l_]:=Sqrt[k] l J3;
P4[k_,l_]:=Sqrt[k] l J4;
P5[k_,l_]:=Sqrt[k] l J5;
P6[k_,l_]:=Sqrt[k] l J6;
P7[k_,l_]:=2 Sqrt[k] l f17[k,l] Sin[2 Pi Sqrt[k] u[t]]+2 Sqrt[k] l f7[k,l] Cos[2
   Pi Sqrt[k] u[t]];
P8[k_,l_]:=2 Sqrt[k] l f18[k,l] Sin[2 Pi Sqrt[k] u[t]]+2 Sqrt[k] l f8[k,l] Cos[2
   Pi Sqrt[k] u[t]];
P9[k_,l_]:=2 Sqrt[k] l f19[k,l] Sin[2 Pi Sqrt[k] u[t]]+2 Sqrt[k] l f9[k,l] Cos[2
   Pi Sqrt[k] u[t]];
P10[k_,l_]:=Sqrt[k] l J10;
P11[k_,l_]:=Sqrt[k] l J11;
P12[k_,l_]:=Sqrt[k] l J12;
P13[k_,l_]:=Sqrt[k] l J13;
P14[k_,l_]:=Sqrt[k] l J14;
P15[k_,l_]:=Sqrt[k] l J15;

(*Definition of the force*)

F[t_]:=ev Cos[w t];

(*We normalize the coefficients I_k for each equation*)

JJ1[k_,l_]:=P1[k,l]/P4[k,l];
JJ2[k_,l_]:=P2[k,l]/P4[k,l];
JJ3[k_,l_]:=P3[k,l]/P4[k,l];
JJ4[k_,l_]:=1;
```

```
JJ5[k_,l_]:=P5[k,l]/P4[k,l];
JJ6[k_,l_]:=P6[k,l]/P4[k,l];
JJ7[k_,l_]:=P7[k,l]/P4[k,l];
JJ8[k_,l_]:=P8[k,l]/P4[k,l];
JJ9[k_,l_]:=P9[k,l]/P4[k,l];
JJ10[k_,l_]:=P10[k,l]/P4[k,l];
JJ11[k_,l_]:=P11[k,l]/P4[k,l];
JJ12[k_,l_]:=P12[k,l]/P4[k,l];
JJ13[k_,l_]:=P13[k,l]/P4[k,l];
JJ14[k_,l_]:=P14[k,l]/P4[k,l];
JJ15[k_,l_]:=P15[k,l]/P4[k,l];

QQ1[k_,l_]:=P1[k,l]/P11[k,l];
QQ2[k_,l_]:=P2[k,l]/P11[k,l];
QQ3[k_,l_]:=P3[k,l]/P11[k,l];
QQ4[k_,l_]:=P4[k,l]/P11[k,l];
QQ5[k_,l_]:=P5[k,l]/P11[k,l];
QQ6[k_,l_]:=P6[k,l]/P11[k,l];
QQ7[k_,l_]:=P7[k,l]/P11[k,l];
QQ8[k_,l_]:=P8[k,l]/P11[k,l];
QQ9[k_,l_]:=P9[k,l]/P11[k,l];
QQ10[k_,l_]:=P10[k,l]/P11[k,l];
QQ11[k_,l_]:=1;
QQ12[k_,l_]:=P12[k,l]/P11[k,l];
QQ13[k_,l_]:=P13[k,l]/P11[k,l];
QQ14[k_,l_]:=P14[k,l]/P11[k,l];
QQ15[k_,l_]:=P15[k,l]/P11[k,l];

(*We define the system that we want to solve*)

system = {u''[t]+JJ5[k,l[t]] l''[t]==-alpha l'[t] JJ5[k,l[t]]-alpha
    u'[t]-JJ6[k,l[t]] F[t] l[t]+l[t] JJ7[k,l[t]]+lambda l[t] JJ8[k,l[t]]-1/l[t]
    (JJ1[k,l[t]]+JJ9[k,l[t]]/(12 k l[t]^2))+l'[t]^2/l[t](JJ3[k,l[t]]+2
    JJ5[k,l[t]])+u'[t]^2/l[t] JJ1[k,l[t]]+2 u'[t] l'[t]/l[t](JJ2[k,l[t]]+1),
l''[t]+QQ5[k,l[t]] u''[t]==-alpha l'[t]-alpha u'[t] QQ5[k,l[t]]-QQ12[k,l[t]] F[t]
    l[t]+l[t] QQ13[k,l[t]]+lambda l[t] QQ14[k,l[t]]-1/l[t]
    (QQ2[k,l[t]]+QQ15[k,l[t]]/(12 k
    l[t]^2))+l'[t]^2/l[t](QQ10[k,l[t]]+2)+u'[t]^2/l[t] QQ2[k,l[t]]+2 u'[t]
    l'[t]/l[t](QQ3[k,l[t]]+QQ5[k,l[t]])};

(*We state the number of points where the system will be solved, and the
    variables where the values of kappa and epsilon will be stored, depending on
    the type of motion, and on whether or not the solution blows up*)
```

```
kpoints=100;
kx = Array[0.1+(4-0.1)/kpoints (#-1)&,kpoints];
nev=100;
evx = Array[(0.1)/nev (#-1)&,nev];
tolerance=0.001;
kvaluesphl={};
evaluesphl={};
kvaluescha={};
evaluescha={};
kvaluesrot={};
evaluesrot={};
kvaluesblowup={};
evaluesblowup={};

(*We use Shared Variables so that we may parallelize the problem to obtain
   results faster*)

SetSharedVariable[evaluesphl];
SetSharedVariable[kvaluesphl];
SetSharedVariable[evaluescha];
SetSharedVariable[kvaluescha];
SetSharedVariable[evaluesrot];
SetSharedVariable[kvaluesrot];
SetSharedVariable[evaluesblowup];
SetSharedVariable[kvaluesblowup];
SetSystemOptions["ParallelOptions" -> "ParallelThreadNumber" -> 4];

(*We run the simulations for the different values of kappa and epsilon*)

ParallelTable[
sys=With[{k=kx[[kval]],ev=evx[[evalue]]},Evaluate[system]];
{usol,lsol}=NDSolveValue[Join[sys,{u[0]==0,u'[0]==0,l[0]==1,l'[0]==0}],{u,l},{t,0,60
   T}];
Xpo=Table[usol[n T],{n,30,60}];
lm=LinearModelFit[Xpo,x,x];
R2=lm["RSquared"];
(*Even if the linear fit is very poor, we need to calculate the average velocity
   to check if we have chaotic motion or not; the fit might be poor due to the
   solution blowing up*)
Which[(R2>=0.7),
velav=First@Pick[lm["BestFitParameters"],lm["BasisFunctions"],x],
True,
```

```
velav=(usol[60 T]-usol[30 T])/(30 T);
];


Which[(velav>=-tolerance && velav<=tolerance),
max=First[FindMaximum[{usol[t],55 T<=t<=57 T},{t,56 T}]];
min=First[FindMinimum[{usol[t],55 T<=t<=57 T},{t,56 T}]];
maxdisp=max-min;
avl=1/Sqrt[kx[[kval]]];
Which[maxdisp>=2 avl,
AppendTo[evaluesrot,evx[[evalue]]];
AppendTo[kvaluesrot,kx[[kval]]];
];
];
(*If the solution blows up, then we cannot take it as showing net transport,
   hence we set the velocity to zero*)
Which[(velav>10^2||velav<-10^2),
AppendTo[evaluesblowup,evx[[evalue]]];
AppendTo[kvaluesblowup,kx[[kval]]];
velav=0;
];

(*We check for net transport, and store the results as appropriate for each type
   of motion*)

Which[(velav>tolerance||velav<-tolerance),
Which[(R2>=0.995),
AppendTo[evaluesphl,evx[[evalue]]];
AppendTo[kvaluesphl,kx[[kval]]],
True,
AppendTo[evaluescha,evx[[evalue]]];
AppendTo[kvaluescha,kx[[kval]]];
];
];
,{kval,kpoints},{evalue,nev}
]

(*We save the data into .txt files so that we can easily recover the results*)

Export["kvaluesphl.txt",kvaluesphl];
Export["evaluesphl.txt",evaluesphl];
Export["kvaluescha.txt",kvaluescha];
Export["evaluescha.txt",evaluescha];
```

```
Export["kvaluesrot.txt",kvaluesrot];
Export["evaluesrot.txt",evaluesrot];
Export["kvaluesblowup.txt",kvaluesblowup];
Export["evaluesblowup.txt",evaluesblowup];
```